Comparison of solar absorption FTIR measurements of CO, NH_3, CH_2O and C_2H_6 with GEOS-Chem model simulations for the Polarstern cruise ANT XX-3

Bachelor thesis

Philipp Richter
2367958

University of Bremen
Institute of Environmental Physics

Date: 22.8.2013
Supervisor: Dr. T. Warneke
1st Examiner: Prof. J. Notholt
2nd Examiner: PD Dr. A. Ladstätter-Weißenmayer

Contents

1 Abstract

The atmospheric gases CO, NH_3, CH_2O and C_2H_6 retrieved by solar absorption *FTIR* spectrometry during the cruise ANT XX-3 of RV Polarstern are compared to *GEOS Chem* simulations. The cruise was a meridional transect on the Atlantic. It started on the 25th January 2003 in Cape Town (South Africa) and ended on the 16th February in Bremerhaven (Germany). During this cruise, the ship crossed a biomass burning plume at about 6° N, resulting in a strong increase of CO, NH_3 and CH_2O concentrations. For carbon monoxide and ammonia model and measurements agree well at all latitudes. The formaldehyde model simulation is significantly lower than the measurements. After scaling with the empirically determined factor 3.7, the results of model and measurements agree well. The ethane's southern hemispheric total columns agree well with the model, while the northern hemispheric values do not agree.

2 Introduction

Within this bachelor thesis the atmospheric gases CO, CH_2O, C_2H_6 and NH_3 measured by solar absorption *FTIR* spectrometry have been compared with simulations using the the atmospheric chemistry model *GEOS Chem*, developed at Harvard University, Massachusetts. While the *FTIR* retrievals were provided, the model runs as well as the comparisons were part of this work.

First, a short introduction is given, which includes topics relevant for the thesis, namely atmospheric layers, the atmospheric circulation in the troposphere and biomass burning. During the cruise of *Polarstern* biomass burning appears between 13° N and 2° N at the african continent. The atmospheric circulation is important for the atmospheric transport of the air masses measured on the ship.

The second part deals with the solar absorption *FTIR* spectrometer and the *GEOS Chem* model.

In the third part, the results of the solar absorption *FTIR* spectrometry and the *GEOS Chem* simulations are presented and discussed.

The fourth part gives a short summary of the results.

2.1 Atmospheric layers

The atmosphere is a gas shell that covers the surface of the earth. It has different layers like the *troposphere*, *stratosphere*, *mesosphere* and the *thermosphere*. The lowest part of the atmosphere is the *troposphere*. It is characterized by decreasing temperature and extends from the surface to about 10 kilometers height at the poles and 18 kilometers height in the tropics. The temperature in *troposphere* decreases, because the main heat source is earth's surface. Human activities and biomass burning influence troposheric

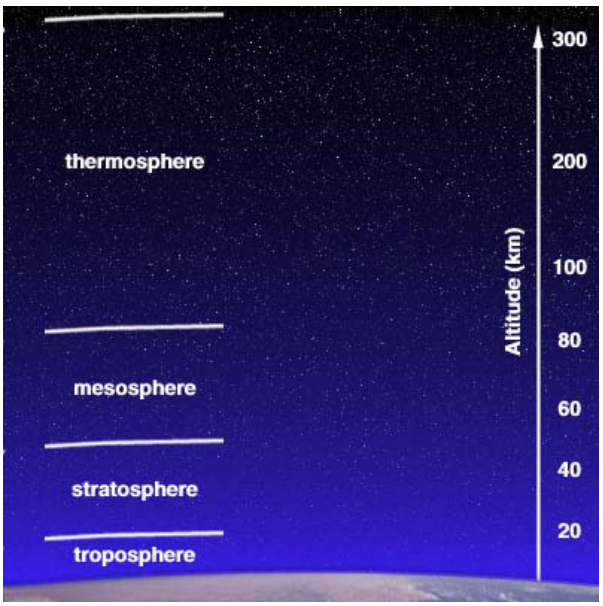

Figure 2.1: Atmospheric layers[2]

chemistry by releasing trace gases to the atmosphere. The border between the *troposphere* and the next layer, the *stratosphere*, is called *tropopause*. Between these two layers only little exchange of gases take place. Nevertheless, tropospheric gases can reach the *stratosphere* via ascending air in the tropics. The temperature in the *stratosphere* increases, due to the *ozone layer*. In the *mesosphere* the temperature decreases again, and finally in the *thermosphere* the temperature increases to up to 1000 °C[13].

2.2 Circulation in the troposphere

The atmospheric circulation is the latitudinal dependend global wind distribution. The three parts are the *trade winds* near the equator, the *westerlies* in temperate latitudes and the *polar easterlies* in the polar regions. While the *trade winds* and the *polar easterlies* are east winds, the *westerlies* is a west wind region.

Trade winds Near the equator, the solar irradition effects the rise of wet air. At this location, a low-pressure area called *Inner-Tropical Convergence Zone* (ITCZ) occurs. Air flows from the surrounding to the ITCZ and is diverted by the *coriolis effect*. They appear up to 35° south and north. In the northern hemisphere the *trade winds* come from

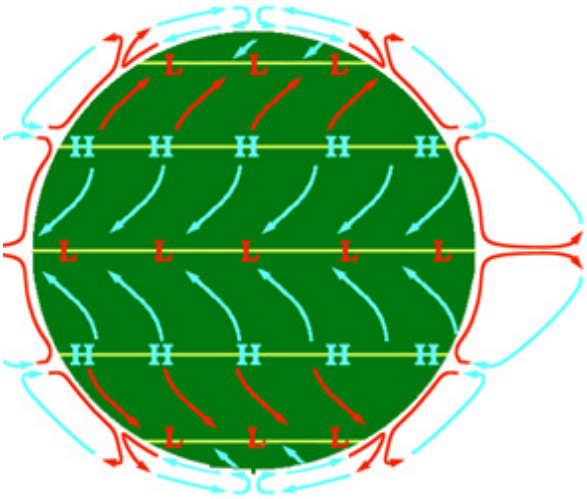

Figure 2.2: Atmospheric circulations[18]

northeast, in the southern hemisphere from southeast. The ITCZ is shifted northwards in northern summer and southwards in southern summer.

Westerlies Between 35° and 70° north and south the *westerlies* appear. The *westerlies* do not show a regular behaviour like the *trade winds*. They can be explained as thermal wind because of the strong temperature gradient between the tropic and the polar zones, superimposed by undulations and disturbances in the atmosphere.

Polar easterlies At the poles, the decending cold air results in a high-pressure area at the ground. This air close to the surface flows towards the low-pressure areas at the edge of the polar circle. Due to the *coriolis effect* the air is directed towards the west and the polar easterlies occur.

2.3 Biomass burning

Biomass burning effects a number of chemical reactions. As mostly known, carbon dioxide and water vapor are produced[1]. Other emitted species are CO, CH_4, C_2H_6, NO_x. Ozone is produced indirectly by photochemical reactions in the plume. Besides chemical reactions there is a large emission of smoke/particles.

The fire dection is performed by the *Moderate Resolution Imaging Spectroradiometer (MODIS)* located on the satellites *Terra* and *Aqua*. *MODIS* uses an algorithm described *Giglio et al. (2003)*[9]. *MODIS* has several channels for detecting reflectances and brightness temperatures. Using this algorithm, *MODIS* is able to tag pixels as *missing data, cloud, water, non-fire, fire* or *unknown*. After finding fire pixels, it is checked if the pixel is tagged as fire due to sun glint. Figure (2.3) shows the fires recognized by *MODIS* for the time of the cruise marked as red dots.

2.4 The Polarstern cruise ANT-XX-3

The cruise started in Cape Town, South Africa (33° S, 18° E) at 25th January 2003 and finished in Bremerhaven, Germany (53° N, 8°) at 16th February 2003. The ship track is shown by the white line in Fig. (2.3). The ITCZ was located around 4° N and 6° N. Large biomass burning activity is recognized by *MODIS* north of the equator. During this cruise, measurments have been performed using a *FTIR* spectrometer from 25th Janaury 2003 to 14th February 2003.[14]

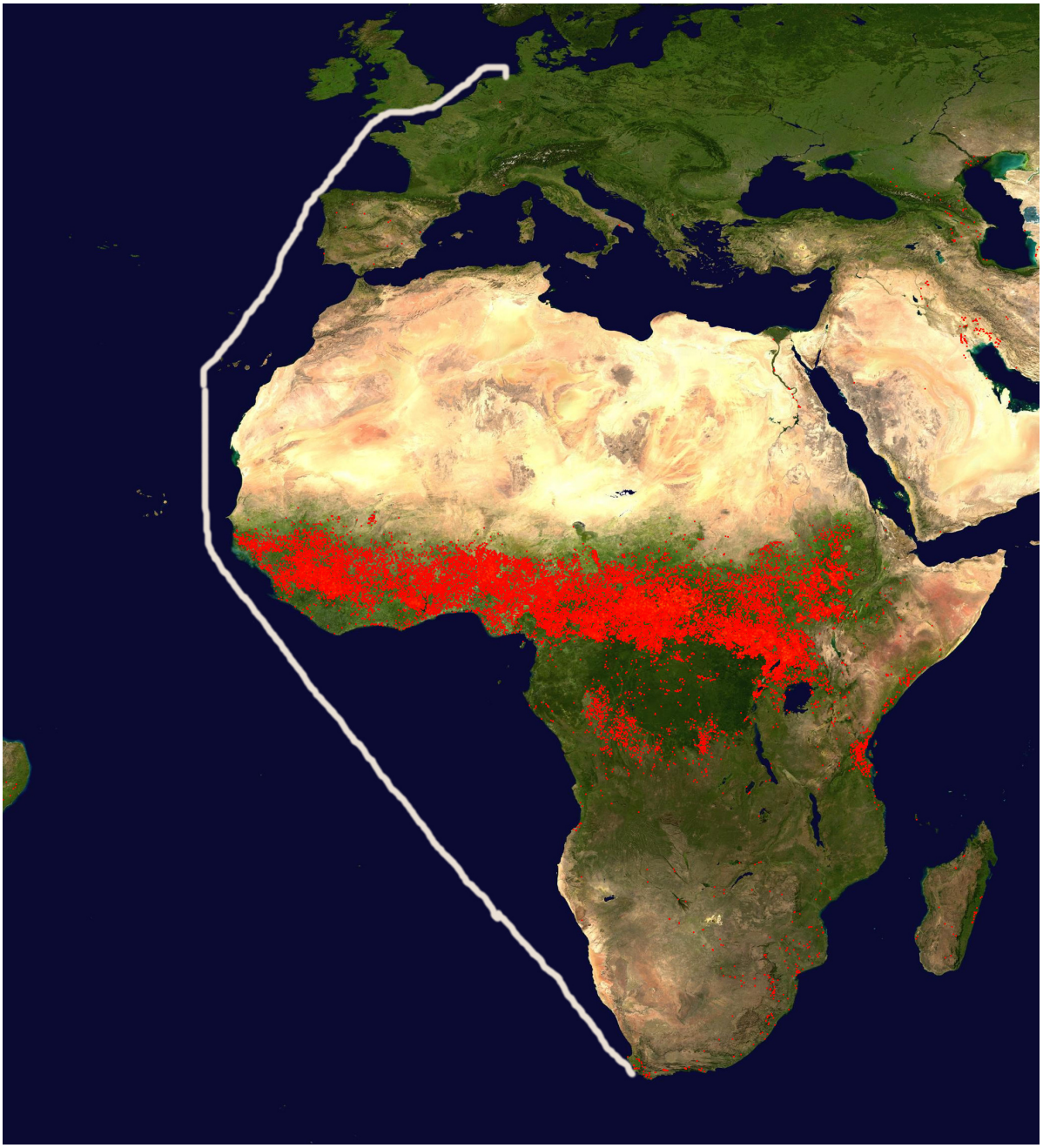

Figure 2.3: Cruise of RV Polarstern and biomass burning. Picture taken from [22]

3 Methods

The measured values are retrieved trace gas concentrations from solar absorption *FTIR (Fourier Transform Infrared)* spectrometric observations. The model values are computed using the *GEOS-Chem* Model. Atmospheric models are an important tool for forecasting the global distribution and propagation of chemical species like *carbon mono/dioxide*, *Methane* or *nitrogenous compounds*. Models have to be validated by measured data.

3.1 Solar Absorption Fourier Transform Spectrometry (FTS)

Solar absorption *FTIR* spectrometry is a remote sensing technique to measure different species in the atmosphere. The important part of the *FTIR spectrometer* is a *Michelson interferometer*. Infrared light is recorded for different optical path differences. From this interferogram, the spectrum is calculated using the *Fourier Transformation*.

3.1.1 Theory of the FTIR spectrometer

Light can be described as plane wave

$$\vec{E}(x,t) = E_0 e^{i(kx-\omega t)} \tag{3.1}$$

where k is the wave number, x the location of the wave, ω the frequency and t the time. If two waves interfere, you need to sum up the wave functions. Using $I = E^2$ the intensity distribution can be computed. The intensity of two interfering waves is

$$I = 2E_0^2(1 + \cos(k(x_1 - x_2))) \tag{3.2}$$

For the *FTIR*, the sun is the light source, so a lot of different frequencies are emitted, so Eq. (3.2) has to be integrated over all wavenumbers:

$$I(x) = \int_0^\infty B(\nu)(1 + \cos(2\pi\nu x))\mathrm{d}\nu \tag{3.3}$$

The $I(x)$ is the measured interferogram. Using a *fourier transformation*, the spectrum ($B_e(\nu)$) can be determined

$$B_e(\nu) = \int_{-\infty}^\infty I(x)\cos(2\pi\nu x)\mathrm{d}\nu \tag{3.4}$$

As known from atomic physics, an atom can absorb photons to lift the shell electren from a low energy level to a higher level. If the electron "falls" down, light with a specific wavelength is emitted. In molecules also *vibrational* and *rotational transitions* exist besides the *electronic transitions*. Vibrational rotational transitions emit light in the infrared region, which is recorded by the *FTIR*. Each molecule has a specific absorption spectrum, so it can be recognized by the absorbed frequencies.

The sum emitts light to the *FTIR spectrometer*. The *Michelson interferometer* consists in general of a beam splitter, a fixed mirror and a moveable mirror. The light enters the interferometer and is splitted by the beam splitter. The light is reflected by the mirrors and behind the beam splitter interferes. Several detectors record the interfered light. The intensity versus the optical path difference is an irregular pattern which is called *interferogram*. So the interferogram will be fourier transformed, resulting in intensity versus wavelength. This is called *spectrogram* or *spectrum*[19]. The spectra were analysed using the line-by-line code *GFIT*, developed at NASA/JPL.[17]

3.2 GEOS-Chem

The *GEOS-Chem* model has been developed at the University of Harvard. It is originally described by *Bey et al. (2001a)*. It is a three-dimensional model of tropospheric chemistry using meteorological observations by the *Goddard Earth Observation System (GEOS)*. Its latitudal-longitudinal resolution is $4° \times 5°$, $2° \times 2.5°$ or $1° \times 1.25°$ and

provides 43 (30 if *gridreduced*) vertical layers.[3] The present work uses the *GEOS-4* meteorological files. The *GEOS-4* files provide the physical quantities displayed in Table (3.1). The given type in the met field describes, in which intervals the given quantity is brought into the simulation.

- A3: Averaged over 3 hours, centered on 1:30, 4:30, ...
- A6: Averaged over 6 hours, centered on 0:00, 6:00, ...
- I6: Instantaneous data at 0:00, 6:00, ...

The *GEOS-Chem* model is implemented in FORTRAN. It is parallelized using *OpenMP*, so it takes advantage of multicore/shared memory CPU's. A parallelization using *MPI* (for computer clusters) has not been implemented yet.
GEOS-Chem provides different options for running the model. The two options used in this work are the *NOx-Ox-Hydrocarbon-aerosol* simulation and the *Tagged CO* simulation.

NOx-Ox-Hydrocarbon-aerosol simulation The *NOx-Ox-Hydrocarbon-aerosol* simulation has 47 tracers, including carbon monoxide (CO), formaldehyde (CH_2O), ethane (C_2H_6), ammonia (NH_3). Methane (CH_4) and carbon dioxide (CO_2) have to be simulated seperately. It includes anthropogenic emissions, biofuel emissions, biogenic emissions and monthly GFED3 biomass emissions. The met fields are given in 3.1. The earliest met fields have to be available one month before simulation start date. Emissions are evaluated every 30 minutes in model time. Dry and wet deposition as sink for gases is enabled. Transport and convection is evaluated every 15 minutes. Chemical reactions are solved every 30 minutes using *SMVGEAR II*. Stratospheric chemistry is linearized. Photolysis frequencies are calculated with the *Fast-J* algorithm by *Wild et al. (2000)*. The output is a binary punch file which has to be read by *GAMAP*. It contains the height layer resolved concentrations for each tracer in the given simulation interval.

Tagged CO simulation The *Tagged CO* simulation uses 17 tracers. This simulation uses the monthly mean OH concentration computed by a previous full-chemistry

Quantity	**Type**	**Dimension**	**Unit**
Land-water-ice flags	I6	2-D	unitless
Surface geopotential heights	I6	2-D	m^2s^{-2}
Surface pressure	I6	2-D	milli bar
Sea level pressure	I6	2-D	milli bar
3-D cloud fraction	A6	3-D	unitless
Hack overshoot parameter	A6	3-D	unitless
Hack convective mass flux	A6	3-D	$kg/m^2/s$
Tendency in specific humidity	A6	3-D	$g\frac{H_2O}{kg}\frac{air}{day}$
Grid box optical depth	A6	3-D	unitless
Specific humidity	A6	3-D	$g\frac{H_2O}{kg}air$
Temperatur	A6	3-D	K
Zonal wind	A6	3-D	ms^{-1}
Meridonal wind	A6	3-D	ms^{-1}
Zhang-McFarlane updraft entrainment	A6	3-D	$Pa \cdot s^{-1}$
Zhang-McFarlane downdraft mass flux	A6	3-D	$Pa \cdot s^{-1}$
Zhang-McFarlane updraft mass flux	A6	3-D	$Pa \cdot s^{-1}$
Surface albedo (visible)	A3	2-D	unitless
Column cloud fraction at ground	A3	2-D	unitless
Top soil wetness	A3	2-D	unitless
Sensible heat flux	A3	2-D	Wm^{-2}
Leaf area indices	A3	2-D	%
Photosynthetically active diffuse radiation	A3	2-D	Wm^{-2}
Photosynthetically active direct radiation	A3	2-D	Wm^{-2}
Planetary boundary layer depth	A3	2-D	m
Total precipitation at ground	A3	2-D	$mm\frac{H_2O}{Day}$
Convective precipitation at ground	A3	2-D	$mm\frac{H_2O}{Day}$
Longwave (IR) radiation emanating from the ground	A3	2-D	Wm^{-2}
Solar insolation (shortwave) reaching the ground	A3	2-D	Wm^{-2}
Snow depth (equivalent water)	A3	2-D	mmH_2O
Air temperature at 2 meter elevation	A3	2-D	K
Skin temperature (ground T or sea surface T)	A3	2-D	K
UWND at 10 m altitude	A3	2-D	ms^{-1}
Friction velocity	A3	2-D	ms^{-1}
VWND at 10 m altitude	A3	2-D	ms^{-1}
Rougness height	A3	2-D	m

Table 3.1: Physical quantities provided by *GEOS-4* met fields[8]

simulation[21]. In this simulation, the CO concentration is tagged for different sources and regions like *fossil fuel burning*, *biomass burning* or *volatile organic compounds oxidation*. Biogenic emissions and dry deposition are disabled, the evaluation timesteps are the same as in the previous *NOx-Ox-Hydrocarbon-aerosol* simulation.

3.3 Comparison

The true state x of the molecules in the atmosphere and the retrieved profile $\bar{x}$ are related by

$$\bar{x} = x_a + A(x - x_a) + \epsilon \tag{3.5}$$

x_a describes the *a priori*, A the *averaging kernel* and ϵ is an error term. The *a priori* values are obtained for example by a soaring balloon. The *averaging kernels* are, if the retrieved state vector is a total column, represented as a vector. It links the true state vector and the retrieved state vector. A depends on model parameters like the solar zenith angle.[12]

The *GEOS-Chem* model produced output is in dimension *ppB (parts per billion)*, whereas the retrieval produced by *GFIT* is given in *Molecules* $\cdot cm^{-2}$. The aim is to compare the total columns of the different species, so the model output has to be converted into *Molecules* $\cdot cm^{-2}$. For this purpose one needs to know the air density. The air density is simulated by the *GEOS-Chem* model and, for there are no geographical informations in it, averaged over the whole earth. The standard deviation is about 1% of the averaged value, so the assumption of a constant air density over the whole earth per height layer seems adequate. The total column of the model data is computed using

$$\bar{x}_{Apriori} = x_{Apriori} \cdot \rho_{Air} \tag{3.6}$$

$$\bar{c} = \rho_{Air} \cdot (c_{geos} - x_{Apriori}) \tag{3.7}$$

$$\bar{x} = \bar{x}_{Apriori} + \bar{c} \tag{3.8}$$

The *GEOS-Chem* height grid is different to the one of the *A priori*, so it was necessary to interpolate the model data to the *A priori* grid. For this reason, a linear interpolation was performed. For interpolating, the function *interp1d* provided by *Scipy* was used.

GEOS Chem gives the model output in the *NetCDF*-format. Using *GAMAP*, the output is convert into an ASCII format. This ASCII file contains the model output in a *column major* description for a 3rd-order tensor with the sizes 144 (longitude) $\times$ 91 (latitude) $\times$ 30 (height):

```
def columnmajor(lines):
    values = [[[0 for x in range(30)] for y in range(91)] for z in range(144)] #Dims: 144, 91, 30
    loop = 0
    for i in range(30):
        for j in range(91):
            for k in range(144):
                try:
                    values[k][j][i] = lines[loop]
                except IndexError:
                    print(loop)
                    print("{} {} {}".format(k,j,i))
                    exit(-1)
                loop = loop + 1

    return values
```

The *GEOS Chem* manpage provides the approriate latitude, longitude and height to each element of the tensor[7]. The program reads these grids (containing the center of the cells) and writes the model values to one textfile per heightlayer.

```
lines = inputASCII()
values = columnmajor(lines)
date = extractDate(sys.argv[1])
vertGrid = getVertGrid()
horGrid = getHorGrid()
saveVals(values, vertGrid, horGrid, date)
```

The next step is to extract the model values at the places, where measured values exist. For this purpose, the measured values are read and the corresponding model values are returned. The earlier produced model files (one file per heightlayer) are read and the content is stored. After this the model values are interpolated to the *Polarstern height grid* (0 to 70 kilometers). The output is stored in one file per day

```
layer0 = gm.getModel(0, modelname, date)

indices = smv.searchModellValues(layer0, latGrid, lonGrid, retr, date)
for index in indices:
    for i in range(30):
        layer = gm.getModel(i, modelname, date)
        val.append(layer[0][index])
    interpolated = li.linearInterpolating(val, vertGrid)
    st.store(interpolated, layer[1][index], layer[2][index], index, modelname, date)
    val = []
```

The *a priori* and the *averaging kernels* are read and combined with the model output. The interpolated air density is multiplied by the *a priori* and added up. The same

procedure is carried out for the gas concentrations. The last step is to add the *a priori* and the processed concentrations, which are stored as total column of the *GEOS Chem*.

```
for i in range(71):
    nh3apr_raw.append(interpolatedChem[i] - apriori[i])

nh3apr = np.asarray(nh3apr_raw)

for i in range(71):
    x_a_col = x_a_col + interpolatedAir[i] * (apriori[i]) #Apriori Column
    nh3ad = nh3ad + (nh3apr[i]*ak[i]) * interpolatedAir[i]

f.write("{}\t{}\tLat: {}\tLon: {}\n".format(date, str((x_a_col + nh3ad)*10**(-4)), lat, lon)) #Write
    total column to file
```

4 Results and discussion

4.1 Carbon Monoxide

Carbon monoxide (CO) is a colourless, odorless and toxic gas[4]. It is produced by incomplete combustion, otherwise carbon dioxide is produced. Furthermore it is produced by methane oxidation ($60\,\mathrm{Tg}\cdot\mathrm{a}^{-1}$)

$$\mathrm{CH_4} + 6\,\mathrm{O_2} \longrightarrow \mathrm{CO} + 2\,\mathrm{H_2O} + 3\,\mathrm{O_3} \tag{4.1}$$

The reaction is the net reaction, in fact more reactions happen. Other sources are Non-methane-hydrocarbon oxidations ($600\,\mathrm{Tg}\cdot\mathrm{a}^{-1}$). Also the ocean releases carbon monoxide to the atmosphere ($50\,\mathrm{Tg}\cdot\mathrm{a}^{-1}$). The most important sink of CO is the depletion by hydroxyl radicals (OH·)

$$\mathrm{CO} + \mathrm{OH}\cdot \longrightarrow \mathrm{CO_2} + \mathrm{H} \tag{4.2}$$

Its atmospheric lifetime is about a few months.[13]

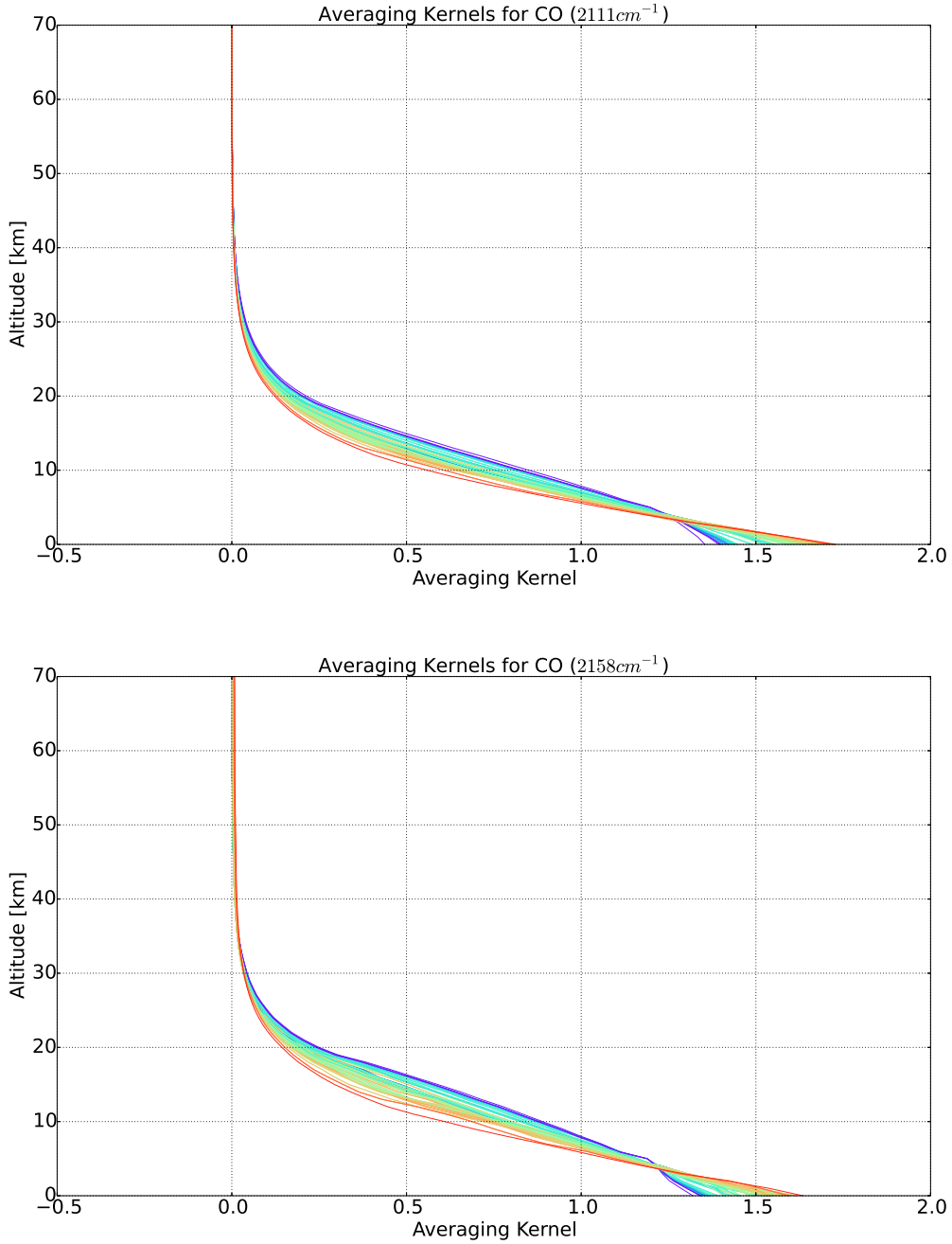

Figure 4.1: Averaging kernels for CO. The colours are related to the solar zenith angle. Upper picture: $k = 2111\,\mathrm{cm}^{-1}$; Lower picture: $k = 2158\,\mathrm{cm}^{-1}$

As shown[1] in Fig. (4.1) the averaging kernels for the different days show same values at same heights. The colours go from red ($sza = 0\,^\circ$) to violet ($sza = 90\,^\circ$). The CO

[1] All plots produced using Matplotlib[10]

kernels are nearly 0 above an altitude of 40 km. Carbon monoxide has been retrieved in the two infrared windows at $k_1 = 2111\,\mathrm{cm}^{-1}$ and $k_2 = 2158\,\mathrm{cm}^{-1}$. Representative averaging kernels were taken for computing the total column of the *GEOS Chem* data. This approach is justified, because the averaging kernels hardly differ at various days (Figure 4.1).

In Figure (4.2) the red and the blue dots show the measurements for $2111\,\mathrm{cm}^{-1}$ (red)

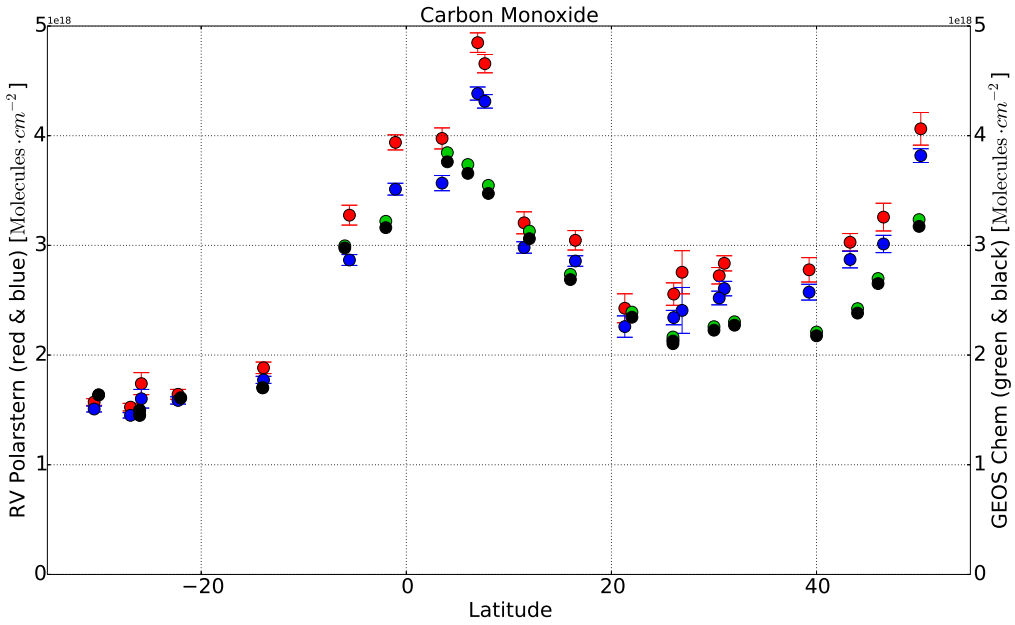

Figure 4.2: CO total column vs latitude. The different datasets are *GEOS Chem* and averaging kernels for $2111\,\mathrm{cm}^{-1}$ (green), *GEOS Chem* and averaging kernels for $2158\,\mathrm{cm}^{-1}$ (black), retrieval for $2111\,\mathrm{cm}^{-1}$ (red) and retrieval for $2158\,\mathrm{cm}^{-1}$ (black), given in $10^{18}\,\mathrm{Molecules}\cdot\mathrm{cm}^{-2}$

and $2158\,\mathrm{cm}^{-1}$ (blue), the black and the green dots show the model values smoothed by the appropriate averaging kernels (green by $2111\,\mathrm{cm}^{-1}$ and black by $2158\,\mathrm{cm}^{-1}$). In the southern hemisphere, the CO concentration is low with about $1.5\times10^{18}\,\mathrm{molecules}\cdot\mathrm{cm}^{-2}$, where model and measurements are nearly the same. Northwards the concentrations increase up to 7° N, where the center of the biomass burning is located. A second increase is at 45 ° N. The retrieval for both infrared windows show same latitudinal variation. The data provided by the *GEOS Chem* model shows the same latitudinal pattern like the retrieval, although the model total column is up to $1.1\times10^{18}\,\mathrm{molecules}\cdot\mathrm{cm}^{-2}$ lower

than the retrieval (Fig. 4.2).

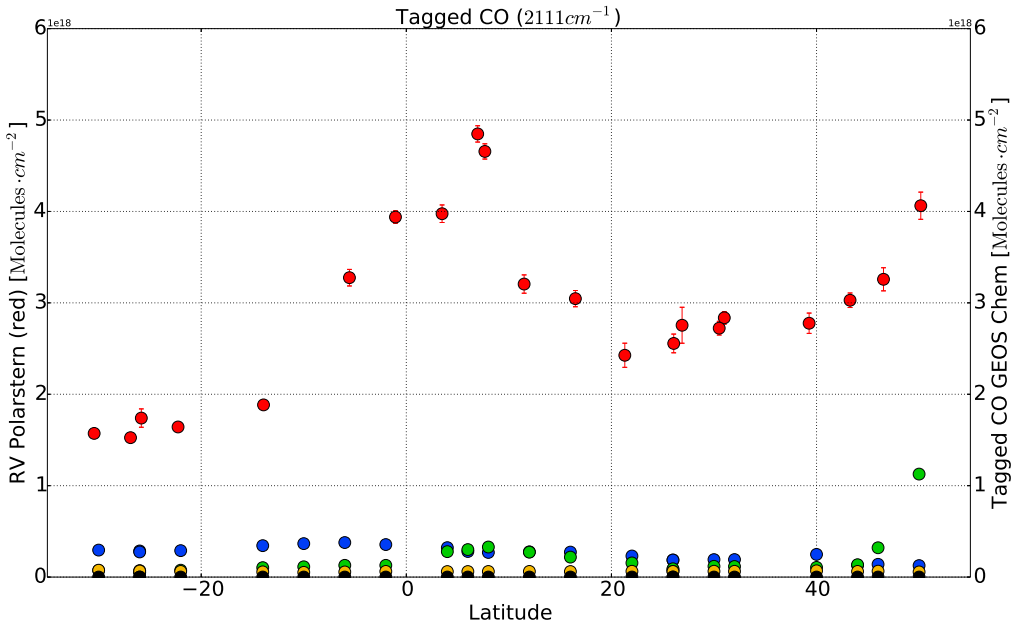

Figure 4.3: Retrieval for $2111\,\mathrm{cm}^{-1}$ and tagged CO for methane (blue), fuel burning (green), biomass burning (yellow) and volatile organic compound oxidation(black), given in $10^{18}\,\mathrm{Molecules}\cdot\mathrm{cm}^{-2}$

Tagged CO In the *Tagged CO* simulation, the CO is "tagged", so it is possible to determine the source of the carbon monoxid. This approach is possible, because the simulation is linear[21]. As shown in Fig. 4.3, the tracers for biomass burning and VOC oxidation are much lower than the retrieved CO. The VOC total column values are about $10 \times 10^{14}\,\mathrm{molecules}\cdot\mathrm{cm}^{-2}$ where isoprene and methanol oxidation has a bigger influence than monoterpene oxidation ($10 \times 10^{13}\,\mathrm{molecules}\cdot\mathrm{cm}^{-2}$). Fuel burning contains biofuel burning and fossil fuel burning except the U.S. and Asia. It shows an increase at $40\,^\circ$ N, west of Europe, so due to wind transport the CO can be carried to the Atlantic Ocean. Figure (4.4) shows the tracers for African biomass burning, U.S. fossil fuel burning and Asian fossil fuel burning. At the equator the same peak in African biomass burning is shown like in Fig. 4.2 which suggests, that the increase is caused by African biomass burning. The trade winds carry the CO from the African continent to the Atlantic Ocean, so the increase is not surprising. North of $20\,^\circ$ N and south of $20\,^\circ$ S there is no impact of African biomass burning on the total CO column. CO emitted by Asian and

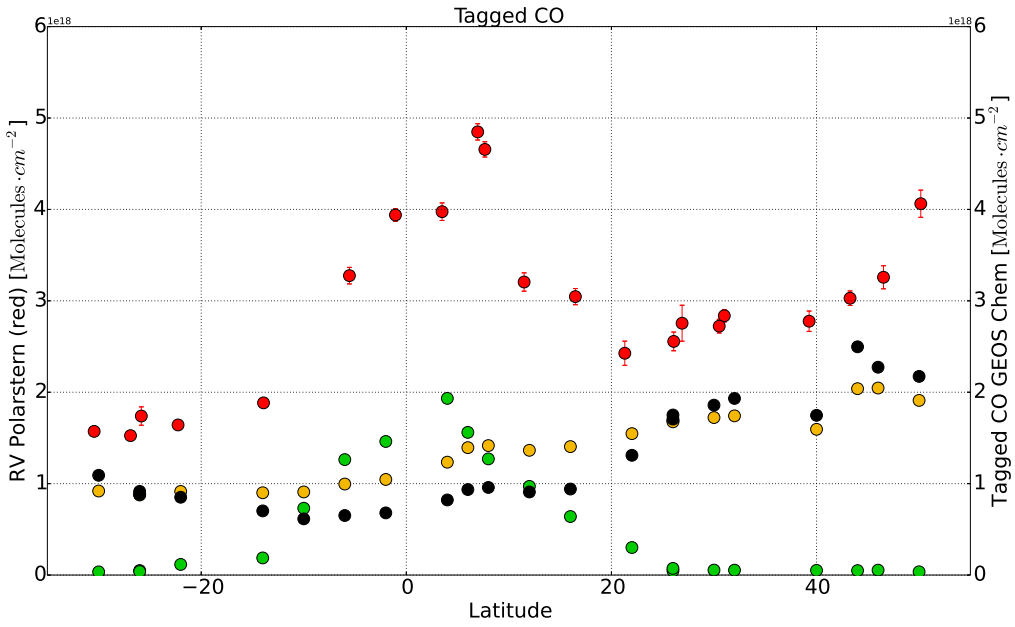

Figure 4.4: Retrieval for 2111 cm^{-1} and tagged CO for African biomass burning (green), U.S. fossil fuel burning (black) and Asian fossil fuel burning (yellow), given in 10^{18} Molecules $\cdot$ cm^{-2}

U.S. fossil fuel burning is increasing from 20 ° S to 40 ° N. It has a lifetime up to 6 months [11], so it is expected to be abudant in the atmosphere. In the northern hemisphere the fossil fuel CO is emitted, and the increase of the retrieval at 40 ° N is caused by the fossil fuel burning.

The Tagged CO simulation considers reactions with OH to be the only sink of CO.[6] It uses "saved OH from a much earlier version of the model, which has been more in line with inferred OH from observations."[2]OH Also the Tagged CO simulation uses other chemical reactions, for example an "outdated VOC chemistry"[2]. Another problem in this special case is an insufficient spin-up time of just one month, so the results of the Tagged CO simulation are strongly influenced by the initial values.

[2]Jenny Fisher, University of Wollongong

4.2 Ammonia

Ammonia (NH_3) is a colourless and toxic gas. Sources of ammonia are mainly fertilization and farming. Further sources are fires and emissions from the ocean and the biosphere. Sinks are deposition and reaction with OH·. Its lifetime is about a few days[5].

The averaging kernels for NH_3 show a nearly day- and sza-independent behaviour, so a representative kernel for each day is chosen (Fig. 4.5).

Measured values and model data show the same latitudinal pattern. North of the

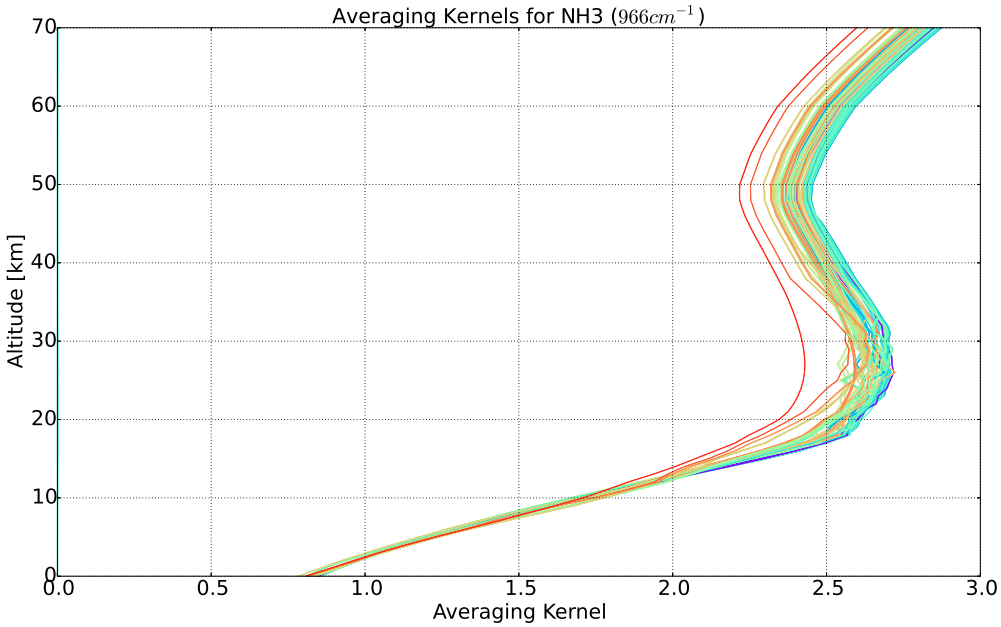

Figure 4.5: Averaging kernels for NH_3 ($966\,cm^{-1}$). The colours are related to the solar zenith angle

equator at 8° N, the model values are only 58% of the retrieved NH_3 values. At 10° S the retrieval is one magnitude above the model. North of 10° N the total columns computed by the model are higher than the retrieved total columns. The model values are 72.58% at 12° N, 68.72% at 16° N and 276.85% at 22° N above the retrieval values.

The ammonia pattern shows lower model values in the southern hemisphere (in Jan-

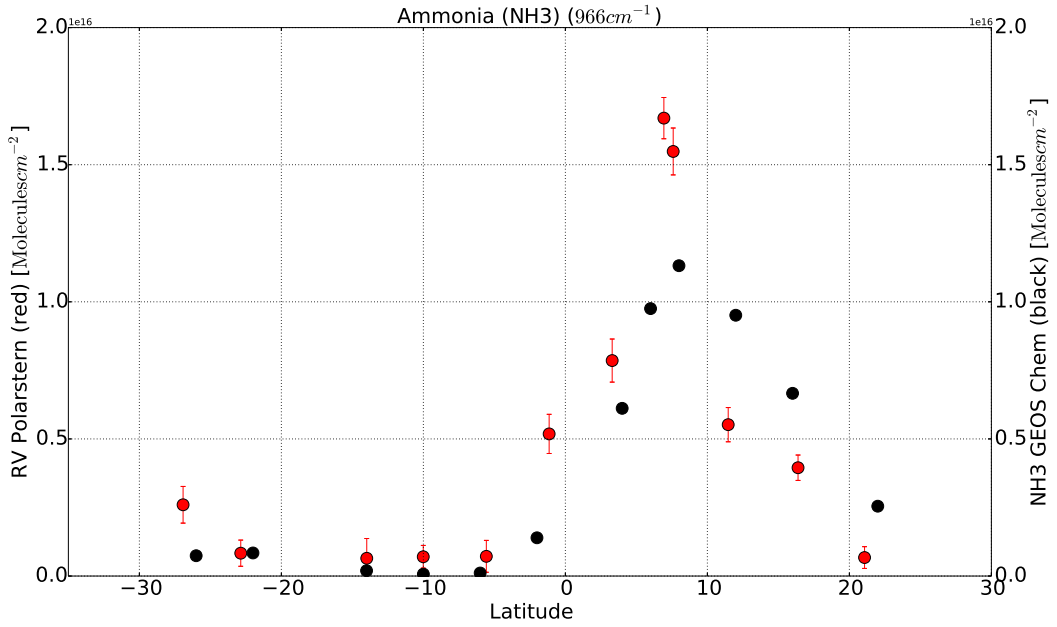

Figure 4.6: Model and retrieval for Ammonia ($966\,\mathrm{cm}^{-1}$), given in $10^{16}\,\mathrm{Molecules}\cdot\mathrm{cm}^{-2}$

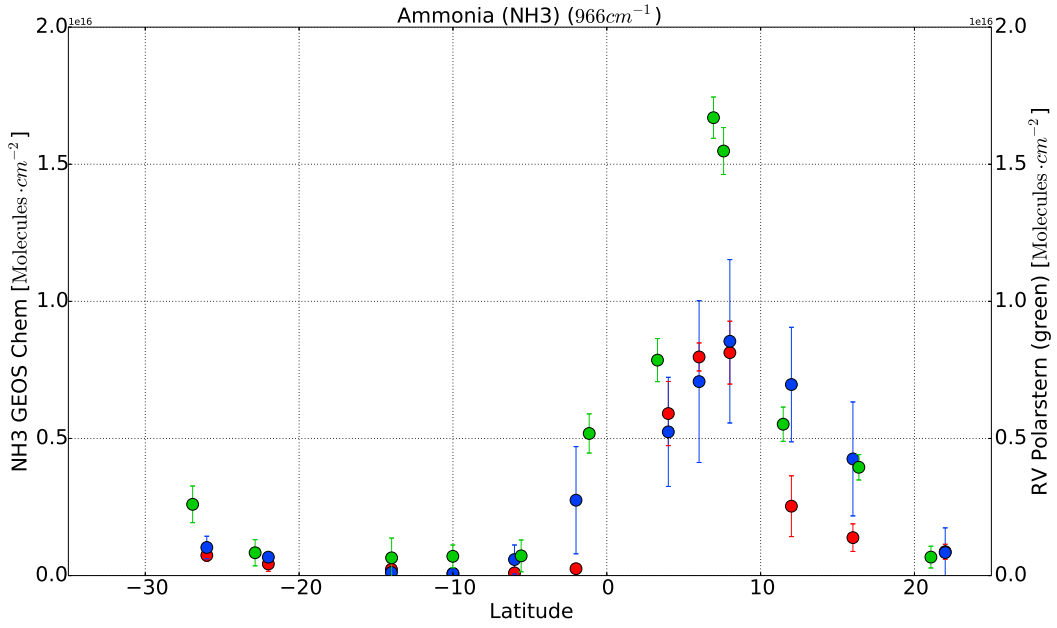

Figure 4.7: Model averaged for every measure site in January (red) and February (blue) versus the retrieval (green), given in $10^{16}\,\mathrm{Molecules}\cdot\mathrm{cm}^{-2}$

uary) and higher measured values in the northern hemisphere (in February). In Figure (4.7) the model values for January and February are plotted seperately. *GEOS Chem* takes the GFED 3 biomass burning emissions for a whole month, so short variations in the burning later in this month influence the concentrations at the beginning of this month. Furthermore, the emissions rapidly changed from January (to 10° S) to February (from 6° S).
In February, the values show a higher spread around the mean, so the standard deviation (the error bars) are much higher than in January. Also the February averages are most of the time higher than the January ones, except from the ITCZ, where the Janaury averages are higher. At southern latitudes without biomass burning influence the January and February averages are nearly the the same with low standard deviation. The high measured values in the ITCZ still above the *GEOS Chem* values.

4.3 Formaldehyde

Formaldehyde (CH_2O) is the most abudant aldehyde in the atmosphere. Its sources are primary methane and NMVOC (Non-Methane volatile organic compounds) oxidations (about 60%), less important sources are biomass burning, fossil fuel combustion. Its sinks are the photolysis reactions $CH_2O \longrightarrow CO + H_2$ and $CH_2O \longrightarrow HCO + H$, and the oxidation by the hydroxil radical $CH_2O + OH \longrightarrow HCO + H_2O$. [16] Its lifetime is a few hours, so it is found near its sources.[20]

The averaging kernels for CH_2O show a nearly day- and sza-independent behaviour, so a representative kernel for each day is chosen (Fig. 7.4).

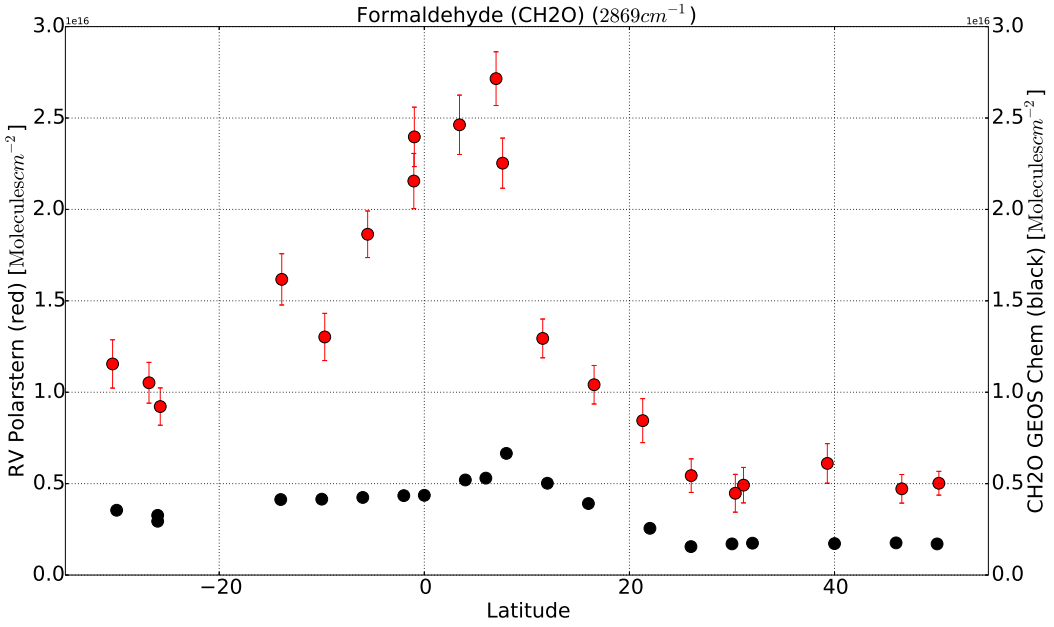

Figure 4.8: Model and retrieval without scaling, given in 10^{16} Molecules $\cdot$ cm^{-2}

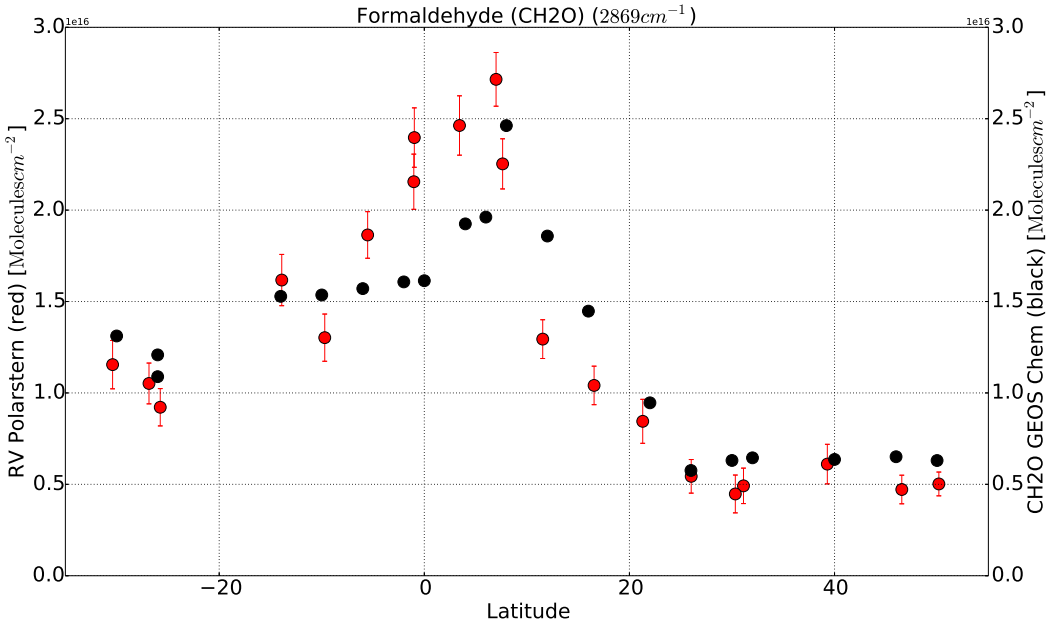

Figure 4.9: Model and retrieval with scaling factor 3.7, given in 10^{16} Molecules $\cdot$ cm^{-2}

Figure (4.8) shows the retrieval and the model values for formaldehyde without any scaling factor. Although the latitudinal variation is the same, the model and the measurements show a large difference in absolute values. The model values are about 30% of the retrieved values, in maximum 39% and in minimum 18%. Figure (4.9) shows the retrieval and the model, where the model is multiplied by a factor 3.7. Low formaldehyde concentration may be caused by to high sinks, meaning an overestimated OH· concentration, or an underestimation of source strengths. Sources of CH_2O are primary oxidation of methane and NMVOC, secondary biomass burning and fossil fuel combustion. The measurements were performed on the ocean, so there are no significant fuel emissions. An underestimation of biomass burning is hardly probable, because the concentration is also to low at places without biomass burning. So the CH_4/NMVOC oxidation, an overestimated OH· concentration or a problem by retrieving CH_2O using solar absorption *FTIR* spectrometry might be the reason for the offset in the formaldehyde values.

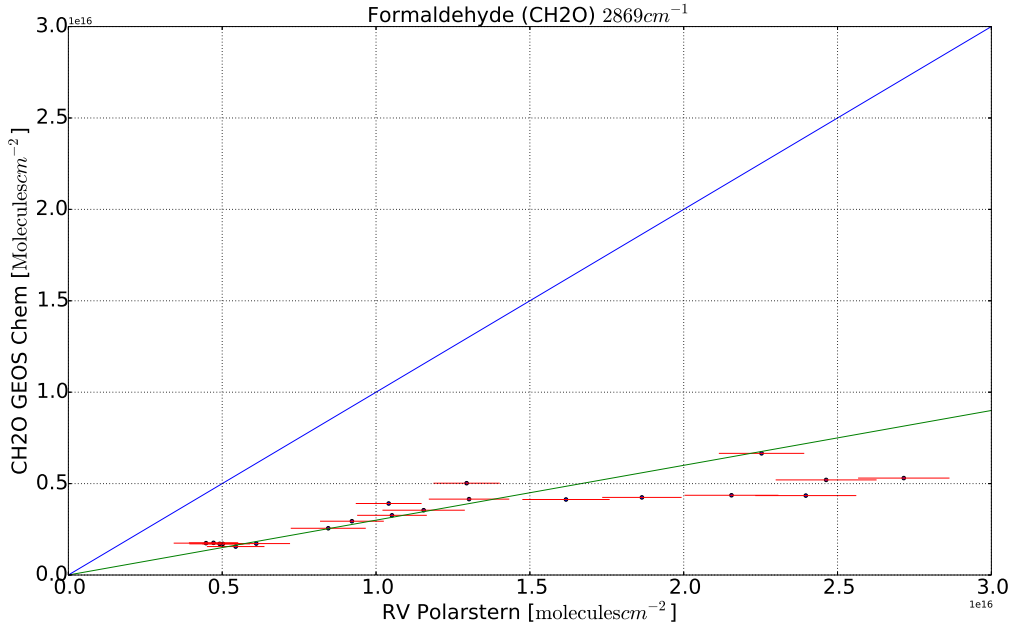

Figure 4.10: Retrieval versus model. The green shows is described by $f(x) = 0.3x$ and shows the correlation between retrieval and model

Figure (4.10) shows the scattering of the solar absorption *FTIR* measurements and the *GEOS Chem* values. The blue line shows perfect agreement ($f(x) = x$) and the green line shows a scaled agreement ($f(x) = 0.3 \cdot x$). This scatterplot reveals, that lower absolute values for CH_2O match better in model and retrieval than higher absolute

values.

4.4 Ethane

After methane, ethane (C_2H_6) is the most abundant hydrocarbon in the remote atmosphere. Its primary sources are fossil fuel ($8.0\,\mathrm{Tg}\cdot\mathrm{yr}^{-1} - 9.2\,\mathrm{Tg}\cdot\mathrm{yr}^{-1}$), biomass burning ($2.4\,\mathrm{Tg}\cdot\mathrm{yr}^{-1} - 2.8\,\mathrm{Tg}\cdot\mathrm{yr}^{-1}$) and biofuel use ($2.6\,\mathrm{Tg}\cdot\mathrm{yr}^{-1}$). Its primary atmospheric sink is reaction with OH·. Most of the sources are located in the northern hemisphere, so due to its short lifetime (two months) and the interhemispheric mixing time (about a year), it has a strong interhemispheric gradient.[15]

For C_2H_6 one averaging kernel deviates significantly from the others (red line). This line belongs to the averaging kernel from 14th February. This value is discarded from the following discussion (Fig. 4.11). For the remaining values, one representative averaging kernel per day is chosen.

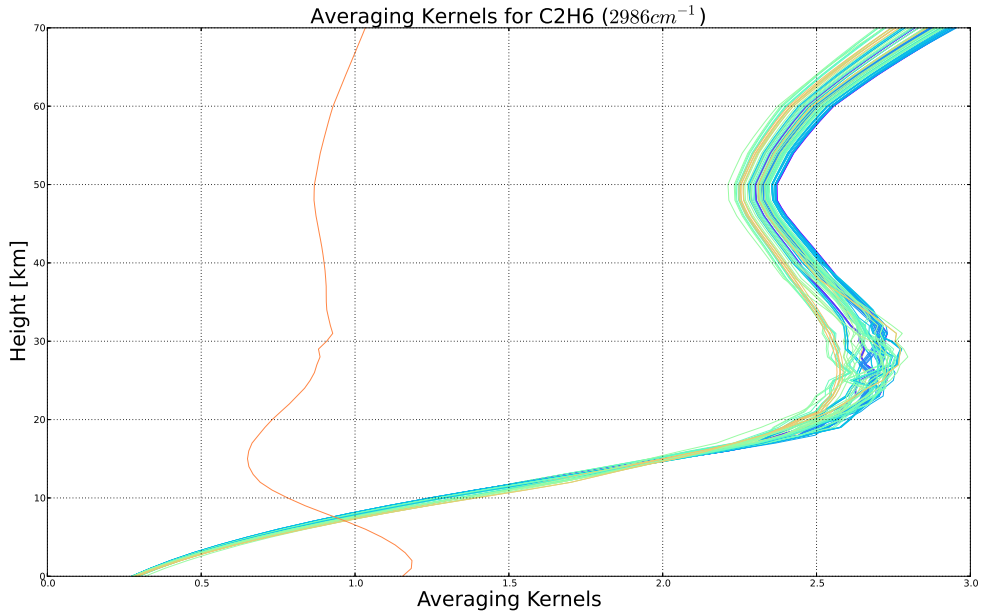

Figure 4.11: Averaging kernels for C_2H_6. The colours are related to the solar zenith angle

Northern hemisphere Figure (4.12) shows ethane's latitudinal variation for the northern hemisphere. Near the equator, the *GEOS Chem* simulations show high total column values. Northwards the total columns decrease until 26° N, slightly increase until 32° N and then decrease until 40° N. The measured values show a different pattern. Near the equator, the total column increases until 7° N. Then the measurement decreases and stays nearly constant at $1.2 \times 10^{16}\,\text{Molecules} \cdot \text{cm}^{-2}$. Finally the measurements increase up to $1.73 \times 10^{16}\,\text{Molecules} \cdot \text{cm}^{-2}$.

The right plot shows the scattering of the values. The red bars are the error bars of the measurements and the green line is described by $f(x) = x$. Only the measurement at $1.21 \times 10^{16}\,\text{molecules} \cdot \text{cm}^{-2}(\text{Measurement})/1.20 \times 10^{16}\,\text{molecules} \cdot \text{cm}^{-2}(\textit{GEOS Chem})$ (16° N) shows good agreement. The other values spread around the green line.

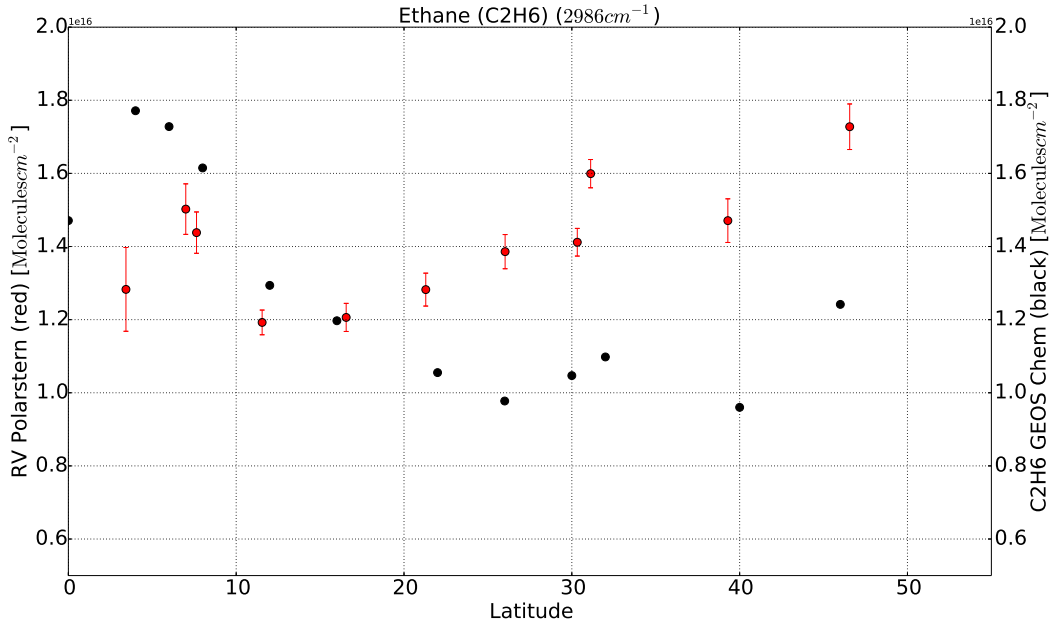

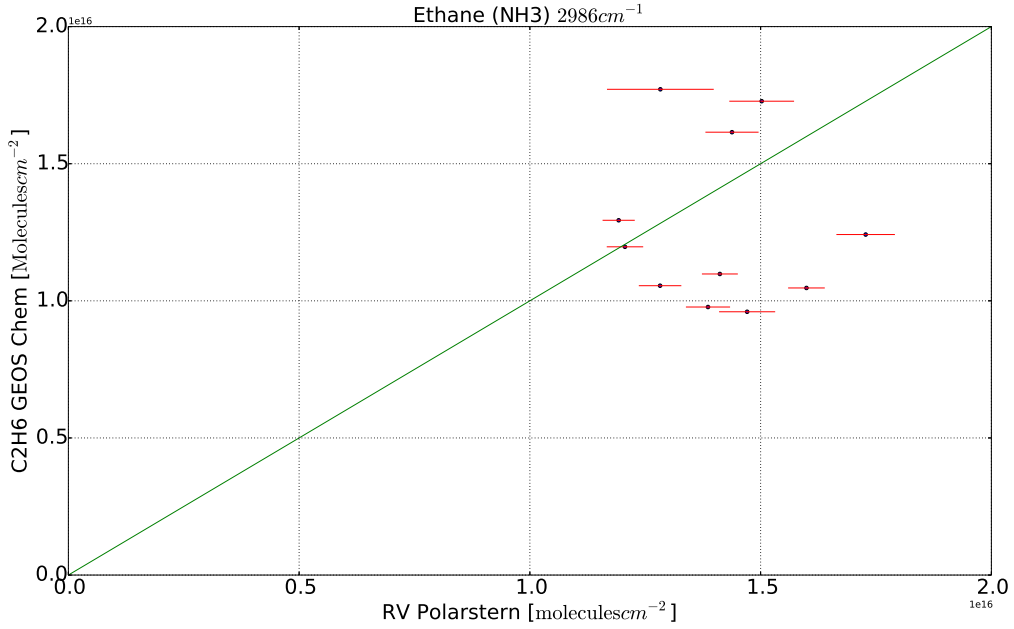

Figure 4.12: Model and retrieval for ethane for the northern hemisphere. Upper picture: Latitude vs. total column, given in 10^{16} Molecules $\cdot$ cm^{-2}. Lower picture: RV Polarstern vs. *GEOS Chem*

Southern hemisphere Figure (4.13) shows ethane's latitudinal variation for the southern hemisphere. At 30° S the measurements and the model show corresponding low concentrations. At this locations, neither biomass burning nor significant fuel burnings (except from ships) happend, also due to the summer on the southern hemisphere, the solar irradiaton was higher than the northern hemispheric ones. Solar irradiation produces the hydroxil radical OH·, which is the primary sink for ethane. Northwards the C_2H_6 concentration increases and reaches its highest value at 6° S where first fires are located (Fig. 2.3). Model and measurements show the same latitudinal pattern, whereby the model overestimates the measurements near the equator. The lower plot shows the correlation between the *GEOS Chem* values and the measurements. The correlation in the southern hemisphere is much better than the correlation at the northern hemisphere, which is shown by the inserted line. The green line is described by $f(x) = x$.

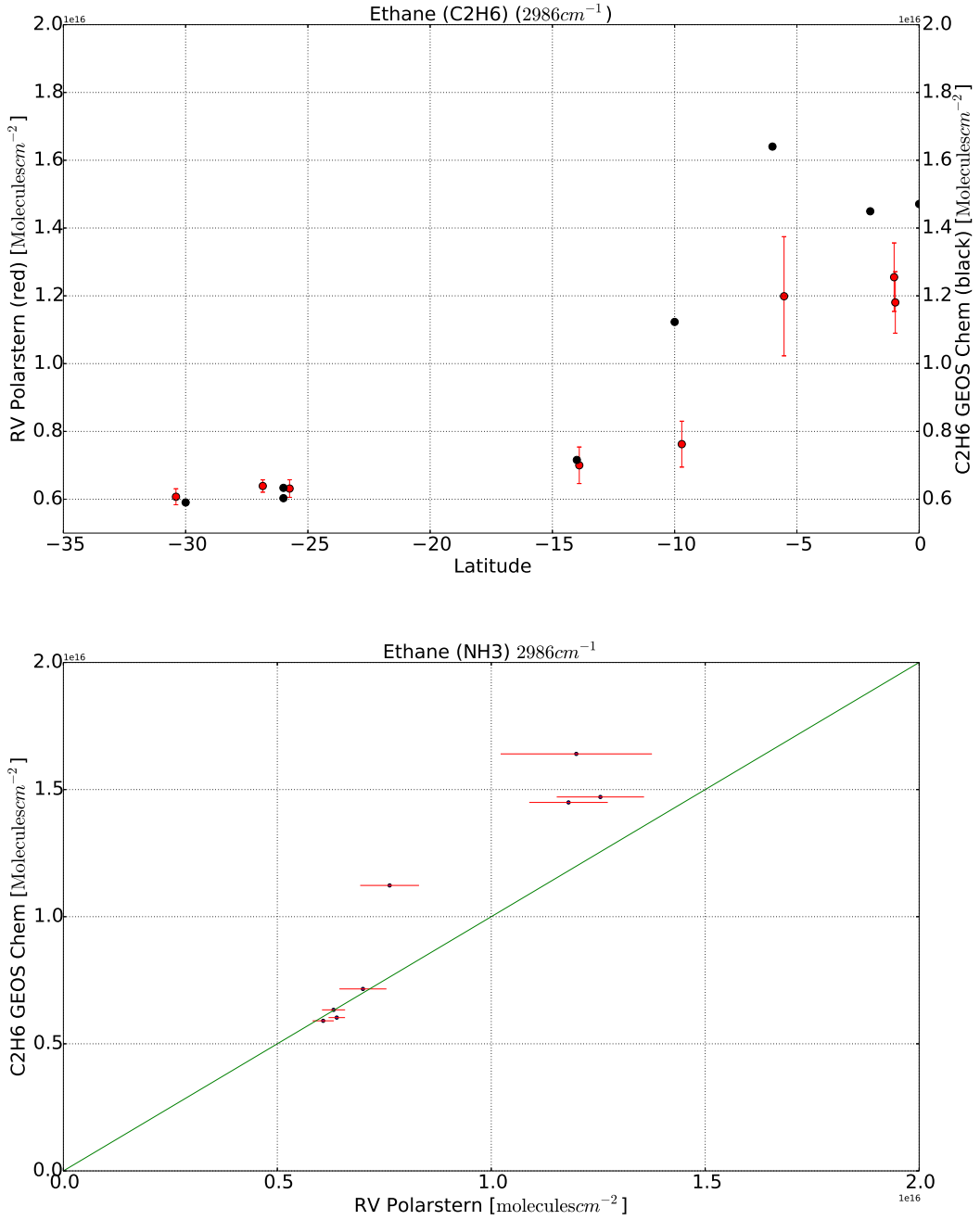

Figure 4.13: Model and retrieval for ethan for the southern hemisphere. Upper picture: Latitude vs. total column, given in 10^{16} Molecules $\cdot$ cm^{-2}; Lower picture: RV Polarstern vs. *GEOS Chem*

The concentrations at the southern hemisphere are not as high as the ones at the northern hemisphere, which is consistent to the statement at the beginning, that the

primary sources of ethane are located at the northern hemisphere.

5 Summary

Carbon monoxide Carbon monoxide shows for both solar absorption *FTIR* spectrometry measurements and *GEOS Chem* simulation values the same latitudinal pattern in absolute values. North of the equator, the biomass burning plume is located. At this place, the model underestimates the retrieved contentration (Fig. 7.2), which can be reasoned by an underestimation of the emitted CO by biomass burning, or an underestimation of OH·. The biomass burning emissions used in the simulation are GFED3 emissions, so if the fire emissions in February decrease, the model also uses in the beginning of the month less fire emissions.
The Tagged CO simulation shows a weak influence of methane oxidation, NMVOC oxidation, fuel burning (except from the US and Asia) and biomass burning (except from Africa). At the equator, a strong influence of African biomass burning is shown (Figure 4.4). In the northern hemisphere, the influence of US and Asian fossil fuel burning grows. A problem with the Tagged CO simulation is, that it the total CO of this simulation and the total CO of the *NOx-Ox-Hydrocarbon-Aerosol* simulation are different, which leads to the assumption, that each simulation uses different chemistry. A further problem is the insufficient spin-up time for the Tagged CO simulation.
Nevertheless, carbon monoxide is a reliable tracer for biomass burning as well as for burning in general.

Ammonia For ammonia, the solar absorption *FTIR* spectrometry measurements and the *GEOS Chem* simulation values show the same latitudinal behaviour, while the model underestimates the retrieval in the southern hemisphere and overestimates it in the northern hemisphere. As in the case of CO inside the the plume the retrieval is higher than the model, while the model shows less decrease than the retrieval in the northern hemisphere. Figure (4.7) shows a large spread around the average value for the model in February and in general higher total columns in February. The northern values of

the retrieval and the February averages show good agreement, while the averages of the equator-near values are less than the values computed at the given date. This lets suppose that the total emissions of NH_3 in *GEOS Chem* in February are decreasing.

Formaldehyde The *GEOS Chem* simulation shows a strong underestimation of CH_2O (Fig. 4.8). Multiplying with the arbitrary factor 3.7, the retrieval and the model show good agreement. In Figure (4.10) the spread is displayed. The correlation is linear, but only at $f(x) = 0.3x$. This underestimation can be reasoned by too low source strengths, whereby each source has to be underestimated. The other reason can be on overestimated OH· concentration, which seems probable, because CO and NH_3 as well show underestimated model values.

Ethane The ethane pattern is split into the northern hemispheric part and the southern hemispheric part. The southern hemispheric part (Fig. 4.13) shows for both solar absorption *FTIR* spectrometry measurements and *GEOS Chem* simulation values the same behaviour, where the southern values up to $10°S$ are nearly the same. The northern hemispheric variation differs to the retrieval and the model, shown in Figure (4.12). Most of the ethane sources are located in the north, which lead s to the assumption of wrong emissions. In the southern hemisphere there are less sources and only few northern-ethane reaches the southern hemisphere due to ethane short lifetime.

In summary, the solar absoprtion *FTIR* measurements and the *GEOS Chem* simulations agree well. The northern hemispheric values for ethane and show a large deviation, while the CH_2O has a large offset. The less high deviation might be reasoned by wrong emissions or overestimated OH· concentrations in the *NOx-Ox-Hydrocarbon-Aerosol* simulation. Nevertheless, the agreement between the solar absorption *FTIR* measurements and the *GEOS Chem*, especially in the biomass burning plume, despite the monthly fire emissions, is remarkable.

6 Acknowledgements

I would like to thank a few persons, without whose help this work would not have been achieved.
First, I thank Prof. Justus Notholt for giving me the chance to write my bachelor thesis in his working group and for beeing my first examiner. As well I thank PD Dr. Annette Ladstätter-Weißenmayer for beeing my second examiner.
From the working group I thank Dr. Thorsten Warneke for his scientific advice and helping me, whenever I got any question. Also I like to thank Dr. Nicholas Deutscher for his scientific advice.
Finally I like to thank Peter Grupe for his technical support and preparing the hardware for smoothly working.

7 Appendix

7.1 Further plots

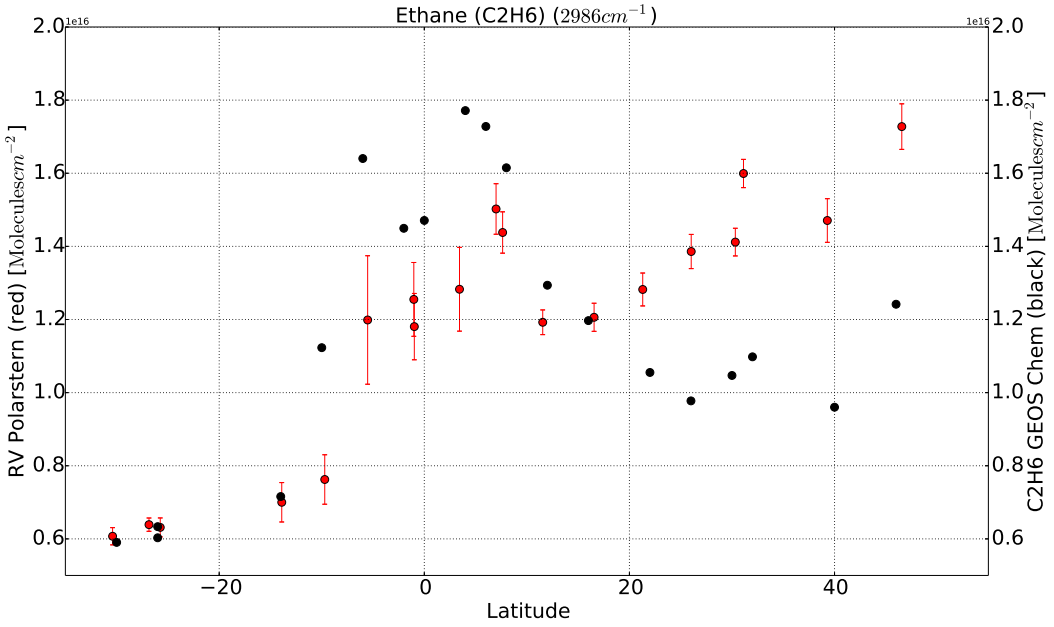

Figure 7.1: Total Ethane

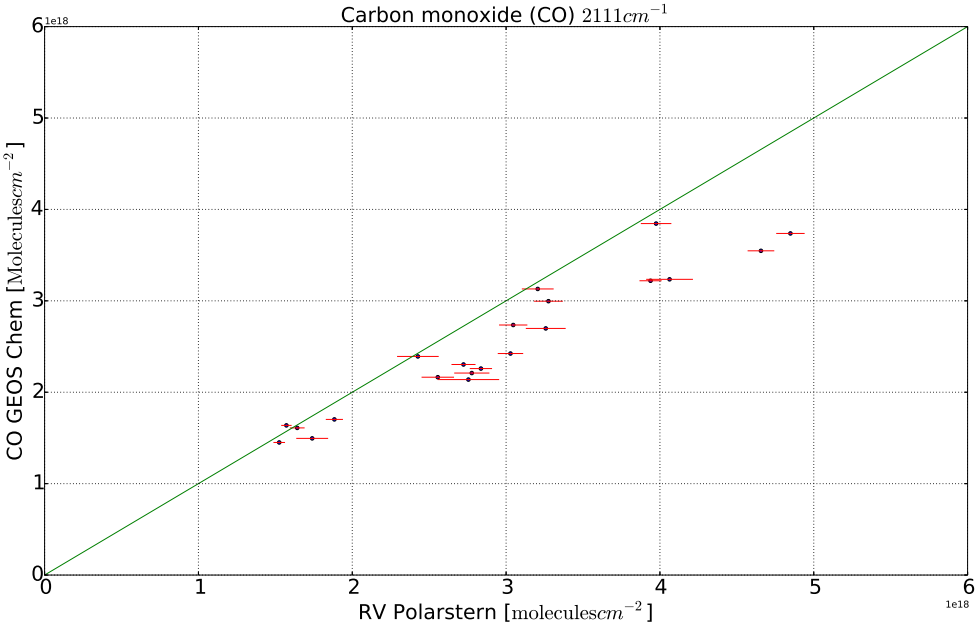

Figure 7.2: CO *GEOS Chem* versus solar absorption *FTIR* spectrometry measurements

7.2 Averaging Kernels

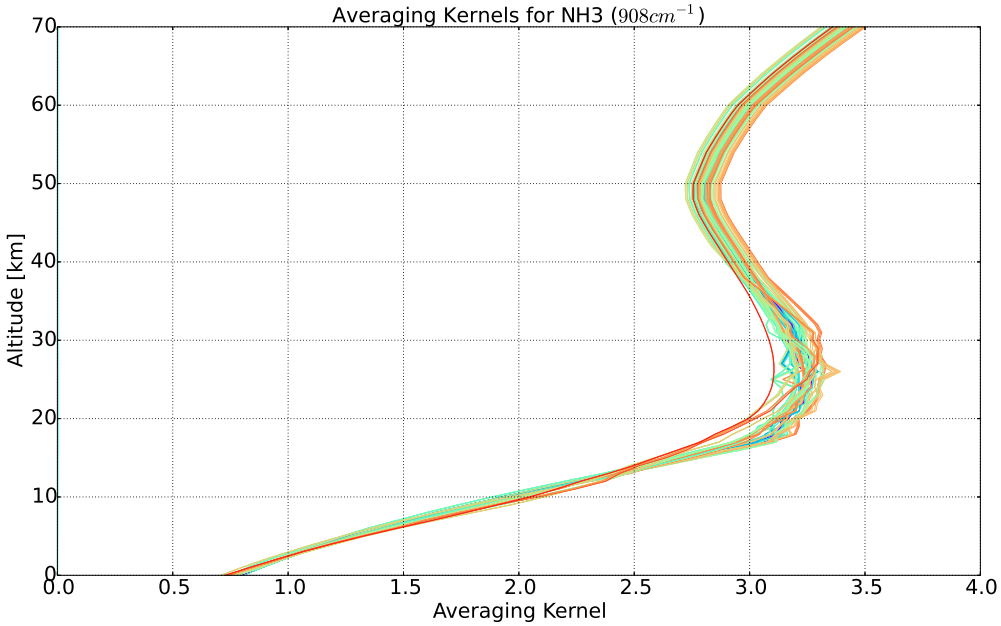

Figure 7.3: Averaging kernels for NH_3 ($908\,cm^{-1}$). The colours are related to the solar zenith angle

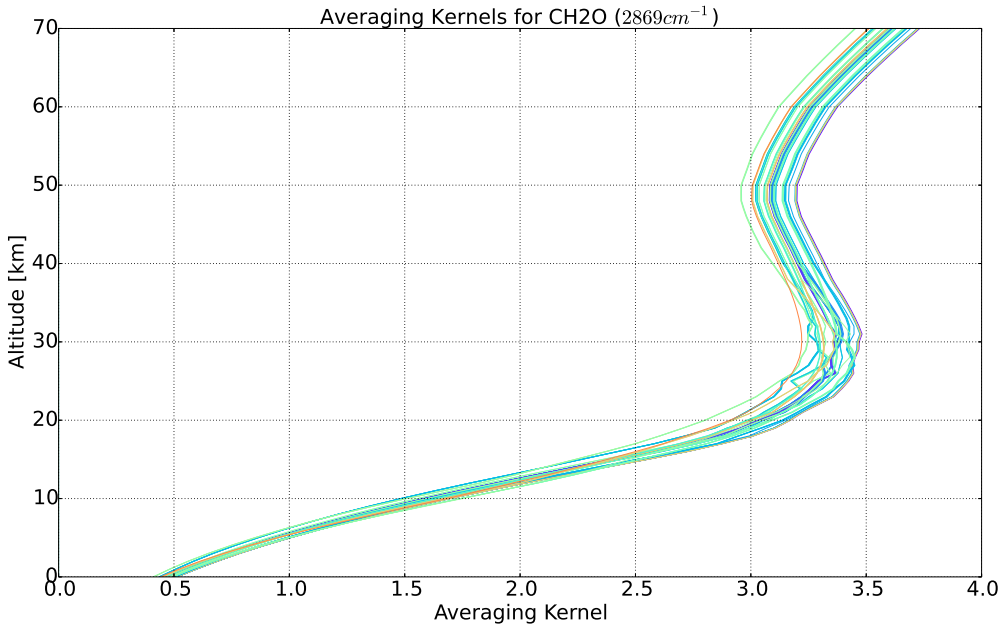

Figure 7.4: Averaging kernels for CH_2O ($2869\,cm^{-1}$). The colours are related to the solar zenith angle

7.3 GFED Emissions

GFED3 emission data can be obtained at `http://www.falw.vu/~gwerf/GFED/GFED3/emissions/` (State 6th August 2013).

7.4 Chemical reactions for NOx-Ox-Hydrocarbon-aerosol simulation

Chemical reactions are listed at `http://acmg.seas.harvard.edu/geos/wiki_docs/chemistry/chemistry_updates_v5.pdf` (State 9th August 2013).

7.5 Processing

Different modules for processing the data:

Sample output of *GEOS Chem*, one reactangle extracted

```
Modeloutput for CO(2003-1-27): Lat=-26.0 Lon=10.0

Height  ppbC
0   56.44068
1   52.1359335739
2   52.2053684334
3   56.0414840917
4   65.0735515657
5   77.5753475204
6   84.599117
7   84.7662676877
8   83.5955057522
9   89.4136904882
10  95.2737672258
11  91.821380129
12  82.2802861596
13  77.8221290649
14  72.7700252317
15  63.6290570233
16  56.2186618164
17  42.5526076592
18  32.5530760377
19  25.5384211522
20  21.6597440541
21  18.1496930586
22  16.5187360989
23  14.8877791392
24  14.8745628859
25  14.894361749
26  15.6970670003
27  16.8466009113
28  17.9961348222
29  19.2896339143
30  20.8552521639
31  22.4208704134
32  23.9864886629
33  25.5521069125
34  27.117725162
35  27.6001189124
36  28.0558759948
37  28.5116330772
38  28.9673901596
39  29.4231472419
40  29.8789043243
41  29.4823644942
42  28.9161828325
43  28.3500011709
44  27.7838195093
45  27.2176378476
46  26.651456186
47  26.0852745243
48  25.2589269074
49  24.3919753552
50  23.5250238031
51  22.6580722509
52  21.7911206988
53  20.9241691466
54  20.0572175945
55  19.2153248887
56  18.4993302421
57  17.7833355956
58  17.067340949
```

```
59   16.3513463025
60   15.6353516559
61   14.9193570094
62   14.2033623628
63   13.4873677163
64   12.8824480806
65   12.2837448923
66   11.685041704
67   11.0863385156
68   10.4876353273
69   9.88893213893
70   9.29022895059
```

Averaging kernel

```
            3            3
 avg_ker    Version 1.2.1     2011-01-05    GCT
Level    AK    Pressure_(atm)
            0    1.6112337         1.0100000
            1    1.5359820        0.89539999
            2    1.4131864        0.79280001
            3    1.3136903        0.70160002
            4    1.2196544        0.61870003
            5    1.1205691        0.54390001
            6    1.0264888        0.47659999
            7   0.93821990        0.41580001
            8   0.85050422        0.36100000
            9   0.76452649        0.31189999
           10   0.67784429        0.26809999
           11   0.59483075        0.22970000
           12   0.51707852        0.19610000
           13   0.44162062        0.16730000
           14   0.37799141        0.14300001
           15   0.32656336        0.12210000
           16   0.28261465        0.10390000
           17   0.24415749       8.81799981E-02
           18   0.20664744       7.46899992E-02
           19   0.17443377       6.33400008E-02
           20   0.14698115       5.38199991E-02
           21   0.12524167       4.57199998E-02
           22   0.10569575       3.88800018E-02
           23  8.99506956E-02    3.31100002E-02
           24  7.64812157E-02    2.82099992E-02
           25  6.43918887E-02    2.40499992E-02
           26  5.48690818E-02    2.05499995E-02
           27  4.65105101E-02    1.75700001E-02
           28  3.96684408E-02    1.50499996E-02
           29  3.35142836E-02    1.29100000E-02
           30  2.83232722E-02    1.11100003E-02
           31  2.39579454E-02    9.61599965E-03
           32  2.06235163E-02    8.33300035E-03
           33  1.77684389E-02    7.23000010E-03
           34  1.52955847E-02    6.28199987E-03
           35  1.32079264E-02    5.46499994E-03
           36  1.14153810E-02    4.76100016E-03
           37  9.87641327E-03    4.15199995E-03
           38  8.55700020E-03    3.62599990E-03
           39  7.42066931E-03    3.17099993E-03
           40  6.44410634E-03    2.77699996E-03
           41  5.60179958E-03    2.43399991E-03
           42  4.87581035E-03    2.13599997E-03
           43  4.24871687E-03    1.87699997E-03
           44  3.70812532E-03    1.65200001E-03
           45  3.24079767E-03    1.45500002E-03
           46  2.89530610E-03    1.28299999E-03
           47  2.71283067E-03    1.13200000E-03
           48  2.10044347E-03    1.00000005E-03
           49  1.52152695E-03    8.83699977E-04
           50  1.26279949E-03    7.80900009E-04
```

```
          51   1.05210592E-03   6.90000015E-04
          52   8.78401217E-04   6.09299983E-04
          53   7.13190879E-04   5.37700020E-04
          54   5.78144041E-04   4.74300003E-04
          55   4.49452142E-04   4.18000011E-04
          56   3.35955905E-04   3.68100009E-04
          57   2.28648656E-04   3.23899993E-04
          58   1.56436727E-04   2.84600013E-04
          59   9.24441774E-05   2.49900011E-04
          60   5.21163784E-05   2.19199996E-04
          61   2.55108353E-05   1.91900006E-04
          62   1.46415787E-05   1.67799997E-04
          63   9.81275844E-06   1.46399994E-04
          64   6.31809962E-06   1.27499996E-04
          65   3.83882343E-06   1.10800000E-04
          66   2.75062212E-06   9.60999969E-05
          67   1.53061296E-06   8.31599973E-05
          68   6.77952698E-07   7.17799994E-05
          69   4.43462426E-07   6.18100021E-05
          70   3.41145011E-07   5.30799989E-05
```

Linear interpolating of the model values

```
import numpy as np
import scipy.interpolate as inter

def linearInterpolating(val, vertGrid):
    height = []
    output = [val[0]]
    for elem in vertGrid:
        height.append(float(elem))

    interpolated = inter.interp1d(height, val)#k lon, j lat
    for i in range(70):
        output.append(np.float(interpolated(i+1)))
    return output
```

Searching for corresponding model values

```
import gridval as gva

def searchModellValues(values, horGridLat, horGridLong, retr, date):

    retrDate = retr[0]
    retrVal = retr[1]
    retrErr = retr[2]
    retrLat = retr[3]
    retrLon = retr[4]

    valVal = values[0]
    valLat = values[1]
    valLon = values[2]

    check = 0
    i = []
    output = []
    #Suche im Retrieval nach dem Datum zu date. Dazu wird jede Zeile von retr untersucht
    for index in range(len(retrDate)):
        test1 = retrDate[index].split(" ")[0].split("-")
        test2 = date.split("-")
        for element in range(len(test1)):
            if(int(test1[element]) == int(test2[element])):
                check = check + 1
        if(check == 3):
            i.append(index)
            check = 0
        else:
            check = 0
```

```
    #exit(-1)

    #Jetzt suche nach den entsprechenden Modellwerten
    for index in i:
        for j in range(len(valLat)):
            if(retrLat[index] < valLat[j] + 1.0 and retrLat[index] > valLat[j] - 1.0 ):
                if(retrLon[index] < valLon[j] + 1.25 and retrLon[index] > valLon[j] - 1.25):
                    output.append(j)

    return output
```

Averaging the measured values to the horizontal *GEOS Chem* grid

```
#!/usr/bin/python2

import numpy as np
import sys

#Lies alle Messwerte und das Grid ein
f = open(sys.argv[1], "r")
cont = f.readlines()
f.close()
f = open("../Grid/gridLatEdge.txt", "r")
latGrid = f.readlines()
f.close()
f = open("../Grid/gridLongEdge.txt", "r")
lonGrid = f.readlines()
f.close()


latitude = []

for element in latGrid:
    elem = element.split(" ")
    for j in range(len(elem)):
        try:
            x = float(elem[j])
        except ValueError:
            pass
        else:
            latitude.append(float(x))

longitude = []

for element in lonGrid:
    elem = element.split(" ")
    for j in range(len(elem)):
        try:
            x = float(elem[j])
        except ValueError:
            pass
        else:
            longitude.append(float(x))

#Werte werden nun korrekt gespeichert
ev = {}
cont = cont[1:]
for element in cont:
    found = False
    x = float(element.split("\t")[3])
    y = float(element.split("\t")[4])
    for i in range(len(latitude)):
        for j in range(len(longitude)):
            if(x <= latitude[i] + 2.0):
                if(y <= longitude[j] + 2.50):
                    key = "{}-{}".format(latitude[i], longitude[j])
                    if(ev.get(key) == None):
                        ev[key] = []
                    ev[key].append(element)
```

```
                    found = True
            if(found):
                break
        if(found):
            found = False
            break

f = open("avNH3_966.txt", "w")
#Jeden einzelnen Eintrag des Dictionarys mitteln
val = []
err = []
lat = []
lon = []
out = []
f.write("Date\tVal\tErr\tLat\tLon\n")
for key in ev.keys():
    for element in ev.get(key):
        val.append(float(element.split("\t")[1]))
        err.append(float(element.split("\t")[2]))
        lat.append(float(element.split("\t")[3]))
        lon.append(float(element.split("\t")[4]))
    out.append("{}\t{}\t{}\t{}\t{}\n".format(ev.get(key)[0].split("\t")[0], np.mean(val), np.mean(err
        ), np.mean(lat), np.mean(lon)))
    val = []
    err = []
    lat = []
    lon = []

sortedOut = []
store = -1
cache = "2005-01-01"
iterate = range(len(out))
for i in iterate:
    for j in range(len(out)):
        if(out[j].split("_")[0] < cache):
            cache = out[j]
            store = j
    sortedOut.append(out[store])
    del out[store]
    cache = "2005-01-01"

for element in sortedOut:
    f.write(element)
f.close()
```

7.6 GEOS Chem values, smoothed with the averaging kernels

C_2H_6

```
2003-01-26 10:34:00 5.90392489607e+15   Lat: -30.0   Lon: 15.0
2003-01-27 13:52:00 6.33462453117e+15   Lat: -26.0   Lon: 10.0
2003-01-27 09:07:00 6.0299887722e+15    Lat: -26.0   Lon: 12.5
2003-01-28 09:21:00 6.96339597698e+15   Lat: -22.0   Lon: 7.5     ##ZU GROSSER FEHLER
2003-01-30 09:37:00 7.15789785591e+15   Lat: -14.0   Lon: 0.0
2003-01-31 08:12:00 1.12295026144e+16   Lat: -10.0   Lon: -2.5
2003-02-01 08:52:00 1.64030315993e+16   Lat: -6.0    Lon: -7.5
2003-02-02 10:47:00 1.4494303224e+16    Lat: -2.0    Lon: -10.0
2003-02-02 10:32:00 1.4709056006e+16    Lat: 0.0     Lon: -10.0
2003-02-03 09:57:00 1.77136399532e+16   Lat: 4.0     Lon: -15.0
2003-02-04 10:29:00 1.72799635853e+16   Lat: 6.0     Lon: -17.5
2003-02-04 10:36:00 1.61498268925e+16   Lat: 8.0     Lon: -17.5
```

```
2003-02-05 10:24:00 1.29373335015e+16   Lat: 12.0   Lon: -20.0
2003-02-06 10:41:00 1.19697654765e+16   Lat: 16.0   Lon: -20.0
2003-02-07 10:41:00 1.05516210971e+16   Lat: 22.0   Lon: -20.0
2003-02-08 09:20:00 9.77439183107e+15   Lat: 26.0   Lon: -20.0
2003-02-09 15:30:00 1.04694190845e+16   Lat: 30.0   Lon: -17.5
2003-02-09 11:06:00 1.09795578077e+16   Lat: 32.0   Lon: -17.5
2003-02-11 14:15:00 9.60098049877e+15   Lat: 40.0   Lon: -12.5
2003-02-12 14:03:00 1.14928510067e+16   Lat: 44.0   Lon: -10.0  ##ZU GROSSER FEHLER
2003-02-13 09:56:00 1.24172290235e+16   Lat: 46.0   Lon: -7.5
```

CH_2O

```
2003-01-26 10:34:00 3.54470948195e+15   Lat: -30.0  Lon: 15.0
2003-01-27 13:52:00 2.94313478606e+15   Lat: -26.0  Lon: 10.0
2003-01-27 09:07:00 3.26526795709e+15   Lat: -26.0  Lon: 12.5
2003-01-28 09:21:00 3.77368575053e+15   Lat: -22.0  Lon: 7.5    ##ZU GROSSER FEHLER
2003-01-30 09:37:00 4.13072103414e+15   Lat: -14.0  Lon: 0.0
2003-01-31 08:12:00 4.1509858276e+15    Lat: -10.0  Lon: -2.5
2003-02-01 08:52:00 4.24505241504e+15   Lat: -6.0   Lon: -7.5
2003-02-02 10:47:00 4.34420513866e+15   Lat: -2.0   Lon: -10.0
2003-02-02 10:32:00 4.36161447872e+15   Lat: 0.0    Lon: -10.0
2003-02-03 09:57:00 5.20205402146e+15   Lat: 4.0    Lon: -15.0
2003-02-04 10:29:00 5.30205982482e+15   Lat: 6.0    Lon: -17.5
2003-02-04 10:36:00 6.65470144985e+15   Lat: 8.0    Lon: -17.5
2003-02-05 10:24:00 5.02214003879e+15   Lat: 12.0   Lon: -20.0
2003-02-06 10:41:00 3.91174043497e+15   Lat: 16.0   Lon: -20.0
2003-02-07 10:41:00 2.55658456106e+15   Lat: 22.0   Lon: -20.0
2003-02-08 09:20:00 1.55611325689e+15   Lat: 26.0   Lon: -20.0
2003-02-09 15:30:00 1.70437656425e+15   Lat: 30.0   Lon: -17.5
2003-02-09 11:06:00 1.74341951924e+15   Lat: 32.0   Lon: -17.5
2003-02-11 14:15:00 1.71950542667e+15   Lat: 40.0   Lon: -12.5
2003-02-12 14:03:00 16106135237.8   Lat: 44.0   Lon: -10.0  ##ZU GROSSER FEHLER
2003-02-13 09:56:00 1.75943762966e+15   Lat: 46.0   Lon: -7.5
2003-02-14 16:16:00 1.70341366869e+15   Lat: 50.0   Lon: 0.0
```

CO 2111 cm^{-1}

```
2003-01-26 09:48:00 1.6373127907e+18    Lat: -30.0  Lon: 15.0
2003-01-27 13:39:00 1.49518646489e+18   Lat: -26.0  Lon: 10.0
2003-01-27 08:51:00 1.45058929272e+18   Lat: -26.0  Lon: 12.5
2003-01-28 09:11:00 1.6098348919e+18    Lat: -22.0  Lon: 7.5
2003-01-30 09:29:00 1.70273614294e+18   Lat: -14.0  Lon: 0.0
2003-01-31 07:53:00 2.31655022143e+18   Lat: -10.0  Lon: -2.5   ##ZU GROSSER FEHLER
2003-02-01 08:44:00 2.99602843973e+18   Lat: -6.0   Lon: -7.5
2003-02-02 10:15:00 3.21956618929e+18   Lat: -2.0   Lon: -10.0
2003-02-03 09:24:00 3.84518528211e+18   Lat: 4.0    Lon: -15.0
2003-02-04 10:15:00 3.73725094055e+18   Lat: 6.0    Lon: -17.5
2003-02-04 12:02:00 3.54713957749e+18   Lat: 8.0    Lon: -17.5
2003-02-05 10:16:00 3.13000881369e+18   Lat: 12.0   Lon: -20.0
2003-02-06 10:20:00 2.73552851591e+18   Lat: 16.0   Lon: -20.0
2003-02-07 10:06:00 2.39170641918e+18   Lat: 22.0   Lon: -20.0
2003-02-08 15:50:00 2.13853272919e+18   Lat: 26.0   Lon: -20.0
2003-02-08 09:55:00 2.16443003564e+18   Lat: 26.0   Lon: -17.5
2003-02-09 15:13:00 2.25891329506e+18   Lat: 30.0   Lon: -17.5
2003-02-09 10:08:00 2.30357543291e+18   Lat: 32.0   Lon: -17.5
2003-02-11 13:58:00 2.20989669216e+18   Lat: 40.0   Lon: -12.5
2003-02-12 13:58:00 2.42342899261e+18   Lat: 44.0   Lon: -10.0
2003-02-13 09:45:00 2.69804642597e+18   Lat: 46.0   Lon: -7.5
2003-02-14 16:06:00 3.23518666589e+18   Lat: 50.0   Lon: 0.0
```

CO 2158 cm^{-1}

```
2003-01-26 09:48:00 1.63659675239e+18   Lat: -30.0  Lon: 15.0
2003-01-27 13:39:00 1.4990972077e+18    Lat: -26.0  Lon: 10.0
2003-01-27 08:51:00 1.45157520879e+18   Lat: -26.0  Lon: 12.5
2003-01-28 09:11:00 1.60900926172e+18   Lat: -22.0  Lon: 7.5
2003-01-30 09:29:00 1.70068841118e+18   Lat: -14.0  Lon: 0.0
```

```
2003-01-31 07:53:00 2.39663950568e+18   Lat: -10.0  Lon: -2.5   ##ZU GROSSER FEHLER
2003-02-01 08:44:00 2.97648158747e+18   Lat: -6.0   Lon: -7.5
2003-02-02 10:15:00 3.16142017153e+18   Lat: -2.0   Lon: -10.0
2003-02-03 09:24:00 3.76171138354e+18   Lat: 4.0    Lon: -15.0
2003-02-04 10:15:00 3.65631421126e+18   Lat: 6.0    Lon: -17.5
2003-02-04 12:02:00 3.47325619092e+18   Lat: 8.0    Lon: -17.5
2003-02-05 10:16:00 3.06114409847e+18   Lat: 12.0   Lon: -20.0
2003-02-06 10:20:00 2.68826330715e+18   Lat: 16.0   Lon: -20.0
2003-02-07 10:06:00 2.34536692357e+18   Lat: 22.0   Lon: -20.0
2003-02-08 15:50:00 2.10376466258e+18   Lat: 26.0   Lon: -20.0
2003-02-08 09:55:00 2.12742158046e+18   Lat: 26.0   Lon: -17.5
2003-02-09 15:13:00 2.22657019088e+18   Lat: 30.0   Lon: -17.5
2003-02-09 10:08:00 2.2721615536e+18    Lat: 32.0   Lon: -17.5
2003-02-11 13:58:00 2.17555693789e+18   Lat: 40.0   Lon: -12.5
2003-02-12 13:58:00 2.38252430787e+18   Lat: 44.0   Lon: -10.0
2003-02-13 09:45:00 2.65175911294e+18   Lat: 46.0   Lon: -7.5
2003-02-14 16:06:00 3.17296314608e+18   Lat: 50.0   Lon: 0.0
```

NH_3 $908\,\mathrm{cm}^{-1}$

```
2003-01-26 08:35:00 6.64214541492e+14   Lat: -32.0  Lon: 15.0
2003-01-27 08:41:00 4.8088682587e+14    Lat: -26.0  Lon: 10.0
2003-01-27 13:30:00 7.03704982392e+14   Lat: -26.0  Lon: 12.5
2003-01-28 07:27:00 8.15853523345e+14   Lat: -22.0  Lon: 7.5
2003-01-30 09:09:00 1.9218729641e+14    Lat: -14.0  Lon: 0.0
2003-01-31 07:42:00 6.54148013854e+13   Lat: -10.0  Lon: -2.5
2003-02-01 08:42:00 1.03939601517e+14   Lat: -6.0   Lon: -7.5
2003-02-02 09:33:00 1.39245301133e+15   Lat: -2.0   Lon: -10.0
2003-02-03 09:09:00 6.05209776909e+15   Lat: 4.0    Lon: -15.0
2003-02-04 11:55:00 9.64932737923e+15   Lat: 6.0    Lon: -17.5
2003-02-04 10:07:00 1.11640755059e+16   Lat: 8.0    Lon: -17.5
2003-02-05 10:08:00 9.26350903333e+15   Lat: 12.0   Lon: -20.0
2003-02-06 09:46:00 6.62245369392e+15   Lat: 16.0   Lon: -20.0
2003-02-06 13:45:00 6.00299401412e+15   Lat: 18.0   Lon: -20.0  ##ZU GROSSER FEHLER
2003-02-07 10:59:00 2.5289129276e+15    Lat: 22.0   Lon: -20.0
2003-02-11 14:47:00 2.0562476449e+14    Lat: 40.0   Lon: -12.5
```

NH_3 $966\,\mathrm{cm}^{-1}$

```
2003-01-27 08:41:00 7.40916748382e+14   Lat: -26.0  Lon: 12.5
2003-01-28 07:27:00 8.4132172326e+14    Lat: -22.0  Lon: 7.5
2003-01-30 09:09:00 1.94747707995e+14   Lat: -14.0  Lon: 0.0
2003-01-31 07:37:00 6.96225583225e+13   Lat: -10.0  Lon: -2.5
2003-02-01 08:36:00 1.09803297863e+14   Lat: -6.0   Lon: -7.5
2003-02-02 09:33:00 1.39456178852e+15   Lat: -2.0   Lon: -10.0
2003-02-03 09:09:00 6.11553225899e+15   Lat: 4.0    Lon: -15.0
2003-02-04 11:55:00 9.75241082339e+15   Lat: 6.0    Lon: -17.5
2003-02-04 10:07:00 1.13170321312e+16   Lat: 8.0    Lon: -17.5
2003-02-05 10:08:00 9.51014121031e+15   Lat: 12.0   Lon: -20.0
2003-02-06 09:46:00 6.6630045369e+15    Lat: 16.0   Lon: -20.0
2003-02-06 13:45:00 6.00565239564e+15   Lat: 18.0   Lon: -20.0  ##ZU GROSSER FEHLER
2003-02-07 09:41:00 2.54689027221e+15   Lat: 22.0   Lon: -20.0
```

7.7 Solar absorption FTIR spectrometer measurement, processed by GFIT and smoothed with the averaging kernels

C_2H_6

```
2003-01-26 10:34:00 6.07175e+15 2.35515e+14 -30.3951666667 14.9408333333
2003-01-27 13:52:00 6.314025e+15 2.588175e+14 -25.74875 10.54725
2003-01-27 09:07:00 6.3893e+15 1.81745e+14 -26.846 11.5605
2003-01-28 09:21:00 1.450785e+16 5.2547875e+16 -22.526 7.61 ##ZU GROSSER FEHLER
2003-01-30 09:37:00 7.00095e+15 5.38735e+14 -13.9005 0.047
2003-01-31 08:12:00 7.624325e+15 6.765025e+14 -9.708125 -3.519375
2003-02-01 08:52:00 1.1987e+16 1.75715e+15 -5.525 -7.028
2003-02-02 10:47:00 1.18055e+16 9.0713e+14 -0.975 -10.8295
2003-02-02 10:32:00 1.255e+16 1.00949e+15 -1.024 -10.795
2003-02-03 09:57:00 1.28275e+16 1.14583875e+15 3.431125 -14.484125
2003-02-04 10:29:00 1.5023e+16 6.9115e+14 6.996 -17.473
2003-02-04 10:36:00 1.43797777778e+16 5.6528e+14 7.63622222222 -18.0081111111
2003-02-05 10:24:00 1.19241666667e+16 3.37825e+14 11.546 -20.3225
2003-02-06 10:41:00 1.206075e+16 3.8412e+14 16.554 -20.966
2003-02-07 10:41:00 1.28213333333e+16 4.49943333333e+14 21.2968333333 -20.8648333333
2003-02-08 09:20:00 1.38596666667e+16 4.67641666667e+14 26.0246666667 -19.188
2003-02-09 15:30:00 1.5993e+16 3.8643e+14 31.122 -16.322
2003-02-09 11:06:00 1.4117e+16 3.78296666667e+14 30.3256666667 -16.7383333333
2003-02-11 14:15:00 1.47076666667e+16 5.96996666667e+14 39.2973333333 -11.7896666667
2003-02-12 14:03:00 1.7012e+16 5.3318125e+16 43.283 -9.7 ##ZU GROSSER FEHLER
2003-02-13 09:56:00 1.7276e+16 6.2314e+14 46.558 -6.982
```

CH_2O

```
2003-01-26 10:34:00 1.15476666667e+16 1.32205e+15 -30.3951666667 14.9408333333
2003-01-27 13:52:00 9.216375e+15 1.020395e+15 -25.74875 10.54725
2003-01-27 09:07:00 1.0518e+16 1.1159e+15 -26.846 11.5605
2003-01-28 09:21:00 1.4595e+16 9.769005748e+20 -22.526 7.61 ##ZU GROSSER FEHLER
2003-01-30 09:37:00 1.6174e+16 1.4023e+15 -13.9005 0.047
2003-01-31 08:12:00 1.302325e+16 1.2916125e+15 -9.708125 -3.519375
2003-02-01 08:52:00 1.86415e+16 1.2745e+15 -5.525 -7.028
2003-02-02 10:47:00 2.3968e+16 1.6253e+15 -0.975 -10.8295
2003-02-02 10:32:00 2.1553e+16 1.50955e+15 -1.024 -10.795
2003-02-03 09:57:00 2.4629125e+16 1.6236625e+15 3.431125 -14.484125
2003-02-04 10:29:00 2.7153e+16 1.4692e+15 6.996 -17.473
2003-02-04 10:36:00 2.25301111111e+16 1.37155555556e+15 7.63622222222 -18.0081111111
2003-02-05 10:24:00 1.29435e+16 1.06040166667e+15 11.546 -20.3225
2003-02-06 10:41:00 1.041065e+16 1.053225e+15 16.554 -20.966
2003-02-07 10:41:00 8.44721666667e+15 1.20311666667e+15 21.2968333333 -20.8648333333
2003-02-08 09:20:00 5.43795e+15 9.19255e+14 26.0246666667 -19.188
2003-02-09 15:30:00 4.9172e+15 9.6949e+14 31.122 -16.322
2003-02-09 11:06:00 4.47396666667e+15 1.03443e+15 30.3256666667 -16.7383333333
2003-02-11 14:15:00 6.1071e+15 1.08207666667e+15 39.2973333333 -11.7896666667
2003-02-12 14:03:00 8.4121e+15 1.03980045874e+21 43.283 -9.7 ##ZU GROSSER FEHLER
2003-02-13 09:56:00 4.71715e+15 7.82245e+14 46.558 -6.982
2003-02-14 16:16:00 5.0214e+15 6.5054e+14 50.173 -0.676
```

CO $2111\,\mathrm{cm}^{-1}$

```
2003-01-26 09:48:00 1.57189230769e+18 3.05914615385e+16 -30.4379230769 14.9810769231
2003-01-27 13:39:00 1.739525e+18 1.0042525e+17 -25.83875 10.6265
2003-01-27 08:51:00 1.5252e+18 3.44675e+16 -26.892 11.6035
2003-01-28 09:11:00 1.6422e+18 4.48594e+16 -22.2574 7.3656
2003-01-30 09:29:00 1.88375e+18 5.2511e+16 -13.923 0.0655
2003-01-31 07:53:00 2.064025e+18 3.53113064899e+22 -9.764125 -3.47025 ##ZU GROSSER FEHLER
2003-02-01 08:44:00 3.27545e+18 9.05105e+16 -5.546 -7.008
2003-02-02 10:15:00 3.938925e+18 6.8742e+16 -1.05875 -10.76275
2003-02-03 09:24:00 3.9750875e+18 9.597075e+16 3.487125 -14.53475
2003-02-04 10:15:00 4.8483e+18 8.9169e+16 6.961 -17.4435
2003-02-04 12:02:00 4.65664e+18 8.34615e+16 7.66 -18.0292
2003-02-05 10:16:00 3.20572e+18 1.001768e+17 11.4872 -20.3102
2003-02-06 10:20:00 3.046225e+18 8.873525e+16 16.4845 -20.9675
2003-02-07 10:06:00 2.426575e+18 1.32037625e+17 21.30475 -20.8625
2003-02-08 15:50:00 2.755e+18 1.967175e+17 26.89 -18.736
2003-02-08 09:55:00 2.55601666667e+18 1.02302e+17 26.075 -19.165
2003-02-09 15:13:00 2.8363e+18 6.9117e+16 31.005 -16.384
2003-02-09 10:08:00 2.72306666667e+18 7.49313333333e+16 30.5096666667 -16.6453333333
```

```
2003-02-11 13:58:00 2.777075e+18    1.11115e+17 39.277  -11.8
2003-02-12 13:58:00 3.02845e+18 7.94365e+16 43.2685 -9.71
2003-02-13 09:45:00 3.25775e+18 1.26335e+17 46.529  -7.0075
2003-02-14 16:06:00 4.0626e+18  1.4877e+17  50.165  -0.707
```

CO 2158 cm^{-1}

```
2003-01-26 09:48:00 1.50817692308e+18   2.68763846154e+16   -30.4379230769  14.9810769231
2003-01-27 13:39:00 1.601675e+18    8.500325e+16    -25.83875   10.6265
2003-01-27 08:51:00 1.45035e+18 2.4415e+16  -26.892 11.6035
2003-01-28 09:11:00 1.58642e+18 3.3205e+16  -22.2574    7.3656
2003-01-30 09:29:00 1.77405e+18 3.21335e+16 -13.923 0.0655
2003-01-31 07:53:00 1.88155e+18 3.53112834371e+22   -9.764125   -3.47025    ##ZU GROSSER FEHLER
2003-02-01 08:44:00 2.8667e+18  4.93695e+16 -5.546  -7.008
2003-02-02 10:15:00 3.5124e+18  5.3865e+16  -1.05875    -10.76275
2003-02-03 09:24:00 3.5676125e+18   6.9289875e+16   3.487125    -14.53475
2003-02-04 10:15:00 4.3841e+18  5.9871e+16  6.961   -17.4435
2003-02-04 12:02:00 4.31303e+18 6.15794e+16 7.66    -18.0292
2003-02-05 10:16:00 2.98078e+18 5.20254e+16 11.4872 -20.3102
2003-02-06 10:20:00 2.8574e+18  4.8004e+16  16.4845 -20.9675
2003-02-07 10:06:00 2.259725e+18    9.761e+16   21.30475    -20.8625
2003-02-08 15:50:00 2.40705e+18 2.09109e+17 26.89   -18.736
2003-02-08 09:55:00 2.3417e+18  6.56148333333e+16   26.075  -19.165
2003-02-09 15:13:00 2.606e+18   6.5976e+16  31.005  -16.384
2003-02-09 10:08:00 2.52023333333e+18   6.23545e+16 30.5096666667    -16.6453333333
2003-02-11 13:58:00 2.573375e+18    7.18985e+16 39.277  -11.8
2003-02-12 13:58:00 2.87105e+18 7.6194e+16  43.2685 -9.71
2003-02-13 09:45:00 3.01275e+18 7.87565e+16 46.529  -7.0075
2003-02-14 16:06:00 3.8183e+18  6.2812e+16  50.165  -0.707
```

$\mathrm{NH_3}$ 908 cm^{-1}

```
2003-01-26 08:35:00 9.1851e+13  5.2905e+14  -31.1175    15.6245
2003-01-27 08:41:00 2.7641e+15  6.3193e+14  -26.922 11.632
2003-01-27 13:30:00 1.2968e+14  7.2852e+14  -26.073 10.845
2003-01-28 07:27:00 1.023305e+15    6.0549e+14  -22.86  7.9095
2003-01-30 09:09:00 1.010725e+15    8.61355e+14 -13.9925    0.125
2003-01-31 07:42:00 2.13545e+14 6.845e+14   -10.0085    -3.2585
2003-02-01 08:42:00 5.0492e+14  1.3405e+15  -5.564  -6.991
2003-02-02 09:33:00 3.222675e+15    1.374625e+15    -1.143  -10.68825
2003-02-03 09:09:00 4.67675e+15 1.571625e+15    3.296125    -14.37725
2003-02-04 11:55:00 1.344025e+16    9.7567875e+14   7.593125    -17.97475
2003-02-04 10:07:00 1.34255e+16 1.00276e+15 6.937   -17.4245
2003-02-05 10:08:00 6.06428333333e+15   6.04071666667e+14   11.4668333333   -20.3058333333
2003-02-06 09:46:00 4.16226666667e+15   5.80616666667e+14   16.3853333333   -20.9675
2003-02-06 13:45:00 7.4759e+15  6.963506144e+20 17.1995 -20.9425    ##ZU GROSSER FEHLER
2003-02-07 10:59:00 8.4642e+14  1.1344e+15  21.198  -20.866
2003-02-11 14:47:00 3.4083e+13  7.0438e+14  39.322  -11.775
```

$\mathrm{NH_3}$ 966 cm^{-1}

```
2003-01-27 08:41:00 2.59825e+15 6.68455e+14 -26.922 11.632
2003-01-28 07:27:00 8.3302e+14  4.7762e+14  -22.86  7.9095
2003-01-30 09:09:00 6.4714e+14  7.21173333333e+14   -13.987 0.120333333333
2003-01-31 07:37:00 7.02785e+14 4.132825e+14    -10.0085    -3.2585
2003-02-01 08:36:00 7.185e+14   5.8088e+14  -5.5665 -6.9885
2003-02-02 09:33:00 5.1828e+15  7.140425e+14    -1.143  -10.68825
2003-02-03 09:09:00 7.8573e+15  7.8565625e+14   3.296125    -14.37725
2003-02-04 11:55:00 1.5482875e+16   8.549575e+14    7.593125    -17.97475
2003-02-04 10:07:00 1.66985e+16 7.52085e+14 6.937   -17.4245
2003-02-05 10:08:00 5.51996666667e+15   6.2416e+14  11.4668333333   -20.3058333333
2003-02-06 09:46:00 3.94945e+15 4.62841666667e+14   16.3853333333   -20.9675
2003-02-06 13:45:00 6.6964e+15  6.96350409615e+20   17.1995 -20.9425    ##ZU GROSSER FEHLER
2003-02-07 09:41:00 6.7425e+14  3.9689e+14  21.0695 -20.864
```

References

[1] Andreae, M. O, *Biomass Burning: Its History, Use, and Distribution and Its Impact on Environmental Quality and Global Climate*, Global biomass burning, Levine, J. S. (Editor), 1991 , P. 3-21

[2] Atmospheric layers `http://disc.sci.gsfc.nasa.gov/ozone/additional/science-focus/about-ozone/layers.shtml` (last accessed 20th August 2013)

[3] Bey, I., D. J. Jacob, R. M. Yantosca, J. A. Logan, B. D. Field, A. M. Fiore, Q. Li, Y. Liu, L. J. Mickley, M. G. Schultz (2001a), *Global modeling of tropospheric chemistry with assimilated meteorology: Model description and evaluation*, Journal Of Geophysical Research 106, 23,073-23,095

[4] Description of CO `http://www.epa.gov/airquality/carbonmonoxide/` (last accessed 20th August 2013)

[5] Description of NH_3 `http://www.atdd.noaa.gov/?q=node/98` (last accessed 20th August 2013)

[6] Duncan B. N., J. A. Logan, I. Bey, I. A. Megretskaia, R. M. Yantosca, P. C. Novelli, N. B. Jones, C. P. Rinsland, *Global budget of CO, 1988 - 1997: Source estimation and validation with a global model*, Journal of Geophysikal Research, Vol. 112, D22301, doi:10.1029/2007JD008459, 2007

[7] GEOS Chem grid `http://acmg.seas.harvard.edu/geos/doc/man/appendix_2.html#A2.3` (horizontal grid) and `http://acmg.seas.harvard.edu/geos/doc/man/appendix_3.html#A3.3.2` (vertical grid) (Both 20th August 2013)

[8] GEOS Chem met fields `http://acmg.seas.harvard.edu/geos/doc/man/appendix_4.html#A4.2` (last accessed 20th August 2013)

[9] Giglio, L., J. Descloitres, C. O. Justice, Y. J. Kaufman (2003), *An Enhanced Contextual Fire Detection Algorithm for MODIS*, Remote Sensing of Environment 87, 273-282, doi:10.1016/S0034-4257(03)00184-6

[10] Hunter, J. D. (2007), *Matplotlib: A 2D graphics environment*, Computing in Science & Engineering, Vol. 9, Number 3, Pages 90 - 95, `http://matplotlib.org/` (last accessed 21st August 2013)

[11] Khalil, M.A.K., R.A. Rasmussen, *Carbon Monoxide in the Earth's Atmosphere: Increasing Trend*, Science 6 April 1984, Vol. 224 no. 4644 pp. 54-56, DOI: 10.1126/science.224.4644.54

[12] Rodgers, C. D. (2000), *Inverse Methods for Atmospheric Sounding: Theory and Practice*, World Scientific Publishing Company, Incorporated

[13] Roedel, W., T. Wagner (2011), *Physik unserer Umwelt*, Springer-Verlag Berlin Heidelberg

[14] Schrems, O. (2008): The expedition of the research vessel "Polarstern" to the Antarctic in 2003 (ANT-XX/3) , Berichte zur Polar- und Meeresforschung (Reports on Polar and Marine Research), Bremerhaven, Alfred Wegener Institute for Polar and Marine Research, 581 , 35 p. ., hdl:10013/epic.31338.d001

[15] Simpson, I.J., Andersen, M.P.S., Meinardi S., Bruhwiler L., Blake N.J., Helmig D., Rowland F.S., Blake D.R., *Long-term decline of global atmospheric ethane concentrations and implications for methane*, Nature 23 August 2012, Vol. 488 pp. 490-494, DOI:10.1038/nature11342

[16] Stavrakou, T., Mller, J.-F., De Smedt, I., Van Roozendael, M., van der Werf, G. R., Giglio, L., and Guenther, A.: Evaluating the performance of pyrogenic and biogenic emission inventories against one decade of space-based formaldehyde columns, Atmos. Chem. Phys., 9, 1037-1060, doi:10.5194/acp-9-1037-2009, 2009.

[17] TCCON-Wiki `https://tccon-wiki.caltech.edu/Software/GGG/Description` (last accessed 20th August 2013)

[18] Tropospheric circulation `http://commons.wikimedia.org/wiki/File:AtmosphCircNT.png` (last accessed 21st August 2013)

[19] University of Bremen, Fortgeschrittenenpraktikum Versuch 17 http://praktikum.physik.uni-bremen.de/images/pdf/fp/fp17_03_02_12.pdf (20th August 2013)

[20] Vigouroux, C., Hendrick, F., Stavrakou, T., Dils, B., De Smedt, I., Hermans, C., Merlaud, A., Scolas, F., Senten, C., Vanhaelewyn, G., Fally, S., Carleer, M., Metzger, J.-M., Mller, J.-F., Van Roozendael, M., and De Mazire, M.: Ground-based FTIR and MAX-DOAS observations of formaldehyde at Runion Island and comparisons with satellite and model data, Atmos. Chem. Phys., 9, 9523-9544, doi:10.5194/acp-9-9523-2009, 2009.

[21] Wikipage for the Tagged CO simulationhttp://wiki.seas.harvard.edu/geos-chem/index.php/Tagged_CO_simulation (last accessed 21st August 2013)

[22] MODIS fires http://rapidfire.sci.gsfc.nasa.gov/firemaps/, Picture of 31st January 2003 (last accessed 21st August 2013)